J. Fluid Mech. (1993), *vol.* 256, *pp.* 499–534

Damping and reflection coefficient measurements for an open pipe at low Mach and low Helmholtz numbers

By M. C. A. M. PETERS, A. HIRSCHBERG, A. J. REIJNEN AND A. P. J. WIJNANDS

Faculty of Physics, W&S 1.46, Eindhoven University of Technology, Postbus 513, 5600 MB Eindhoven, The Netherlands

(Received 19 September 1992 and in revised form 1 June 1993)

The propagation of plane acoustic waves in smooth pipes and their reflection at open pipe terminations have been studied experimentally. The accuracy of the measurements is determined by comparison of experimental data with results of linear theory for the propagation of acoustic waves in a pipe with a quiescent fluid. The damping and the reflection at an unflanged pipe termination are compared.

In the presence of a fully developed turbulent mean flow the measurements of the damping confirm the results of Ronneberger & Ahrens (1977). In the high-frequency limit the quasi-laminar theory of Ronneberger (1975) predicts accurately the convective effects on the damping of acoustic waves. For low frequencies a simple theory combining the rigid-plate model of Ronneberger & Ahrens (1977) with the theoretical approach of Howe (1984) yields a fair prediction of the influence of turbulence on the shear stress. The finite response time of the turbulence near the wall to the acoustic perturbations has to be taken into account in order to explain the experimental data. The model yields a quasi-stationary limit of the damping which does not take into account the fundamental difference between the viscous and thermal dissipation observed for low frequencies.

Measurements of the nonlinear behaviour of the reflection properties for unflanged pipe terminations with thin and thick walls in the absence of a mean flow confirm the theory of Disselhorst & van Wijngaarden (1980), for the low-frequency limit. It appears however that a two-dimensional theory such as proposed by Disselhorst & van Wijngaarden (1980) for the high-frequency limit underestimates the acoustical energy absorption by vortex shedding by a factor 2.5.

The measured influence of wall thickness on the reflection properties of an open pipe end confirms the linear theory of Ando (1969). In the presence of a mean flow the end correction δ of an unflanged pipe end varies from the value at the high-Strouhal-number limit of $\delta/a = 0.61$, with a the pipe radius, which is close to the value in the absence of a mean flow given by Levine & Schwinger (1948) of $\delta/a = 0.6133$, to a value of $\delta/a = 0.19$ in the low-Strouhal-number limit which is close to the value predicted by Rienstra (1983) of $\delta/a = 0.26$.

The pressure reflection coefficient is found to agree with the theoretical predictions by Munt (1977, 1990) and Cargill (1982*b*) in which a full Kutta condition is included. The accuracy of the theory is fascinating in view of the dramatic simplifications introduced in the theory. For a thick-walled pipe end and a pipe terminated by a horn the end correction behaviour is similar. It is surprising that the nonlinear behaviour at low frequencies and high acoustic amplitudes in the absence of mean flow does not influence the end correction significantly.

Author	Theory	Exp.	$\|R\|$	δ	α	ka	M	Sr_0	Sr_{ac}
Munt (1977, 1990)	×	—	×	—	—	var.	< 1	var.	$\gg 1$
Rienstra (1983)	×	—	×	×	—	< 1	< 1	$\ll 1$	$\gg 1$
Cargill (1982*a*, *b*)	×	—	×	—	—	< 1	< 1	$\ll 1$	$\gg 1$
Ando (1969) Levine & Schwinger (1948) Nomura (1960)	×	—	×	×	—	var.	0	—	$\gg 1$
Kirchhoff (1868) Tijdeman (1975)	×	—	—	—	×	var.	0	—	$\gg 1$
Howe (1979*b*, 1984)	×	—	×	×	×	< 1	< 1	$\gg 1$	$\gg 1$
Ronneberger (1975) Ronneberger & Ahrens (1977)	×	×	—	—	×	var.	< 1	var.	$\gg 1$
Ingard & Singhal (1974, 1975)	×	×	×	—	×	< 3.5	< 0.5	var.	$\gg 1$
Disselhorst & Wijngaarden (1980)	×	×	×	—	—	< 1	0	—	var.
Ingard & Ising (1967) Bechert (1980) Cummings & Eversman (1983) Cummings (1984)	×	×	×	—	—	var.	< 1	var.	< 1
Alfredson & Davies (1970) Abrishaman (1977) Davies (1980) Abom & Boden (1986, 1988)	—	×	×	×	—	> 0.1	< 0.2	> 1	$\gg 1$
Peters *et al.* (1992)	—	×	×	×	—	< 0.3	< 0.2	var.	var.

TABLE 1. Summary of existing theoretical and experimental literature on the reflection and damping of acoustic waves in an open pipe; var. denotes a continuous range of values

The aero-acoustic behaviour of the pipe end is dramatially influenced by the presence of a horn. In the presence of a mean flow the horn is a source of sound for a critical range of the Strouhal number.

The high accuracy of the experimental data suggests that acoustic measurements can be used for a systematic study of turbulence in unsteady flow and of unsteady flow separation.

1. Introduction

In duct systems, which are part of complex flow distribution systems, used for example by the Netherlands gas distribution company to distribute gas under high pressure, acoustic excitation can be caused by compressors or flow instability. In particular we study the coupling between periodic vortex shedding and acoustic standing waves. To be able to predict for a given geometry the conditions at which resonant acoustic oscillations occur and to estimate the amplitude of such a resonance, knowledge is required on the quality factor of the resonator. This quality factor is determined by, amongst other things, the reflection coefficient of the acoustic waves at the end of the resonator, the damping of the acoustic waves by visco-thermal losses in the boundary layer and the interaction of acoustic waves with a turbulent mean flow. Typical for industrial conditions are low frequencies, low mean flow velocities and very high Reynolds numbers.

In this paper an open pipe with various types of pipe terminations is studied. A plane acoustic pressure wave of complex-valued amplitude $\hat{p}_+$ and a reflected wave of complex-valued amplitude $\hat{p}_-$ are travelling inside the pipe in positive and negative directions respectively. The reflection coefficient $R = \hat{p}_-/\hat{p}_+$ at an open pipe end is

easily obtained with a two-microphone method as described by Boden & Abom (1986) and Abom & Boden (1988). In the original method the wavenumbers of the plane acoustic waves are assumed to be known. These wavenumbers are calculated from the damping coefficient according to Kirchhoff (1868), see Davies (1988), Boden & Abom (1986), Abom & Boden (1988). A major advantage of the two-microphone method is that data can be obtained for very low Helmholtz numbers (Peters *et al.* 1992), at which the standing-wave method does not yield accurate results (Alfredson & Davies 1970). In order to increase the accuracy of the measurements, the two-microphone method is extended to a multi-microphone method with which the wavenumbers and the reflection properties can be measured simultaneously. In this way, the damping $\alpha_{\pm}$ of acoustic waves travelling in the pipe has also been determined.

The parameters characterizing the problem are the Mach number $M = U_0/c_0$, the Helmholtz number $ka = \omega a/c_0$, the mean flow Strouhal number $Sr_0 = \omega a/U_0$ which is equal to ka/M and the acoustic Strouhal number $Sr_{ac} = \omega a/\hat{u}_{ac}$. Here, a is the inner radius of the pipe, ω the radian frequency of the acoustic waves inside the pipe, U_0 is the mean volume flow divided by the pipe cross-sectional area πa^2 and c_0 is the speed of sound, while $\hat{u}_{ac}$ is the amplitude of the acoustic velocity at the open end of the pipe. Table 1 gives a summary of the main theoretical and experimental literature of the last few decades on the magnitude of the reflection coefficient $|R|$, the phase ϕ of the reflection coefficient R, expressed as a so-called end correction $\delta = (\phi - \pi)/(2\omega/c_0)$ and the damping $\alpha_{\pm}$. Many theoretical results have been obtained for the reflection of acoustic waves at an open pipe end with sharp edges (e.g. Levine & Schwinger 1948), as well as for the influence of wall thickness (e.g. Ando 1969), mean flow (e.g. Munt 1977, 1990; Cargill 1982*a*, *b*; Rienstra 1983; Howe 1979*a*) and vortex shedding (e.g. Disselhorst & van Wijngaarden 1980) on the reflection properties. However, no accurate experimental data are available for cases with both a low Mach number and a low Helmholtz number. In many cases experimental results are given in terms of transmission losses (e.g. Bechert 1980; Cummings & Eversman 1983). Typical scatter in reported data, as for example by Alfredson & Davies (1970), Abrishaman (1977), Ingard & Singhal (1975), Davies, Bento Coelho & Bhattacharya (1980), Boden & Abom (1986), and Abom & Boden (1988) of the reflection of plane acoustic waves at an open pipe end amounts to 3% in $|R|$, the magnitude of the pressure reflection coefficient R and 20% in the end correction δ.

In the absence of a mean flow accurate predictions for the reflection coefficient and end correction at a sharp-edged pipe end are given by Levine & Schwinger (1948). For low Helmholtz numbers $ka < 0.5$, the work of Ando (1969) indicates that in a quiescent fluid there is no significant influence of the wall thickness at the pipe end on the magnitude of the reflection coefficient. However, Ando (1969) also predicted a significant increase of the end correction δ with increasing wall thickness, δ rising to the value of the end correction for a flanged pipe end given by Nomura, Yamamura & Inawashiro (1960).

There is little information on the dependence of the reflection coefficient on the ratio $\hat{u}_{ac}/U_0$ of the amplitude of the acoustic velocity $\hat{u}_{ac}$ at the pipe end and the mean flow velocity U_0 in presence of a mean flow nor on the ratio of the acoustical displacement and the pipe radius $Sr_{ac} = \omega a/\hat{u}_{ac}$ in the absence of mean flow. Some experimental work on the nonlinear behaviour of pipe ends and diaphragms on the reflection characteristics at high acoustic amplitudes has been described in terms of quasi-stationary models by Ingard & Ising (1967), van Wijngaarden (1968), Bechert (1980), Cummings & Eversman (1983) and Cummings (1984). For a quiescent fluid, a prediction for the acoustic energy absorption by vortex shedding was calculated in the

limit $Sr_{ac} \gg 1$ by Disselhorst & van Wijngaarden (1980) using a two-dimensional description of the flow.

In the presence of a mean flow, the reflection coefficient R and damping α are strongly influenced by the Mach number. The influence of the Mach number on the reflection properties was studied using a linear theory, including a Kutta condition at the pipe end, by Munt (1977, 1990). The theory of Munt (1977) and other theories, derived from this basic theory assume a uniform main flow (plug flow) and infinitely thin shear layers as boundaries for the jet. The shear-layer oscillations induced by the acoustic perturbations grow exponentially as they are convected away from the edges of the pipe end. Obviously after a few hydrodynamic wavelengths it is questionable whether linear theory is still applicable. Hence the validity of the theory is not obvious. Furthermore the theory should only be valid when the acoustic boundary layer is large compared to the main flow boundary layer at the pipe exit. The theory of Munt (1990) predicts that the reflection coefficient $|R|$ can exceed unity within a critical range of the Helmholtz number. Cargill (1982*a*, *b*) and Rienstra (1983) analysed the problem for the case of low Strouhal number ($Sr_0 = ka/M$), and found a similar behaviour for the magnitude of the reflection coefficient when the Kutta condition was imposed at the edges of the pipe end, but a significantly different behaviour for the solution in which no Kutta condition was imposed. For the latter solution, the magnitude of the reflection coefficient in the low-Strouhal-number limit is equal to $|R| = (1-M)/(1+M)$ which corresponds to the reflection of all of the acoustic energy at the pipe end. Rienstra (1983) was also able to predict a low-Strouhal-number limit for the end correction in the presence of a low-Mach-number mean flow. It is common practice (e.g. Davies 1988) to assume that for an unflanged pipe termination the presence of a mean flow has no effect on the ratio of the end correction δ and the pipe radius a ($\delta/a = 0.6133$, see Levine & Schwinger 1948), i.e. for low Strouhal numbers it has the same value as for high Strouhal numbers. However, the low-Strouhal-number theory of Rienstra (1983) predicts the much lower value of $\delta/a = 0.2554$. For the high-Strouhal-number limit, Rienstra (1983) and Howe (1979*a*) derived that the end correction indeed approaches the value ($\delta/a = 0.6133$) found in the absence of a mean flow component. For small but finite Mach numbers Howe (1979*a*) found a correction factor, which is a function of the Mach number, which has to be applied to this value of the end correction. In the intermediate region of $Sr_0 = O(1)$ Cargill (1982*b*) states that there is no simple approximate analytical expression for δ/a. There are some indications of the non-uniform behaviour of δ/a for low Mach numbers and low Helmholtz numbers. For example, the experimental data of Davies *et al.* (1980) indicate a decrease of the end correction δ as a result of the presence of a mean flow. However in the latter investigation the different cases of $Sr_0 \to 0$ and $Sr_0 \to \infty$ are not distinguished.

Powell (1951), Wilson *et al.* (1971) and Hirschberg *et al.* (1988) have shown that the presence of a horn at the end of the pipe may have a spectacular influence on the aero-acoustic behaviour of an open pipe termination. For a critical range of the Strouhal number the value of the energy reflection coefficient, defined as

$$R_E = |R|^2(1-M^2)/(1+M)^2,$$

exceeds unity. We will present some additional data in particular on the behaviour of the end correction.

In a quiescent fluid, a theoretical expression for the damping coefficient α is given by Kirchhoff (1868) for the case when the acoustic boundary layer is thin compared to the pipe radius. A general theory for low-frequency plane wave propagation in pipes can

be found in Tijdeman (1975). In the presence of a mean flow, the damping coefficient for the acoustic waves travelling in upstream direction is different from that for waves travelling in the downstream direction. This convective effect on the damping of acoustic waves has been studied by Ronneberger (1975), who proposes a quasi-laminar theory taking the turbulent mean flow profile into account, but neglecting the dissipation due to the interaction of the turbulent stresses and the acoustic field. An important parameter appears to be the ratio of the thickness $\delta_{ac} = (2\nu/\omega)^{\frac{1}{2}}$ of the acoustic boundary layer and the thickness $\delta_l \approx 10\nu/(\tau_0/\rho_0)^{\frac{1}{2}}$ of the viscous sublayer of the turbulent mean flow boundary layer. Here, ν is the kinematic viscosity, ρ_0 is the density of the fluid and τ_0 is the mean wall shear stress. If the ratio is small, $\delta_{ac} \ll \delta_l$, the damping of acoustic waves is not influenced by the turbulent stresses, and a general agreement between the quasi-laminar theory of Ronneberger (1975) and the experimental data has been demonstrated by Ronneberger & Ahrens (1977). For very large values of the ratio δ_{ac}/δ_l, a quasi-stationary theory has been proposed by Ingard & Singhal (1974). A theory including the non-uniform turbulent eddy viscosity is proposed by Howe (1979*b*), and extended in a later paper by Howe (1984). Howe's (1984) theory predicts the global features of the damping coefficient $\alpha_{\pm}$ satisfactorily. However, the difference between the experimental data obtained by Ronneberger & Ahrens (1977) and the results of the theory of Howe (1984) is still quite large, of the order of 20%. Furthermore the theory of Howe (1979*b*, 1984) is based on a two-dimensional flat-plate approximation and does not yield a finite quasi-stationary limit for the damping at low frequencies. Intuitively the ratio δ_{ac}/δ_l is expected to be crucial for the validity of the assumptions of plug flow and Kutta condition in the model of Munt (1977). These assumptions correspond to the limit $\delta_{ac}/\delta_l \gg 1$. For this reason, reflection coefficient measurements have been carried out over a wide range of values, $0.2 < \delta_{ac}/\delta_l < 3$.

The purpose of the present investigation is to obtain accurate data for the reflection coefficient R and the damping $\alpha_{\pm}$ for low Helmholtz numbers ka, low Mach numbers M, and for a wide range of Strouhal numbers $Sr_0 = ka/M$ and Sr_{ac}. In this region of parameters, very few experimental data exist (see table 1) and furthermore this region is of special interest for practical applications. Differences between the various theoretical predictions for R and $\alpha_{\pm}$ are relatively small in this range of the parameters. Therefore a high accuracy of the experimental data is required to validate the predictions.

In §2 the experimental set-up will be described as well as the extension of the two-microphone method to a multi-microphone method. The accuracy of the model is checked by comparison of experimental data, obtained in absence of a mean flow, with predictions.

The damping of acoustic waves due to viscous and thermal forces, the influence of a non-zero mean flow and turbulence will be discussed in §3, where experimental data on the damping coefficient α are also presented.

In §4 the acoustic properties of an open pipe end in the absence of mean flow is studied. The influence of the pipe end geometry on the reflection characteristics of a pipe end is determined and compared with theories found in the literature for both low- and high-amplitude acoustic fields. Finally the influence of a mean flow on the reflection properties of an open pipe end is discussed in §5.

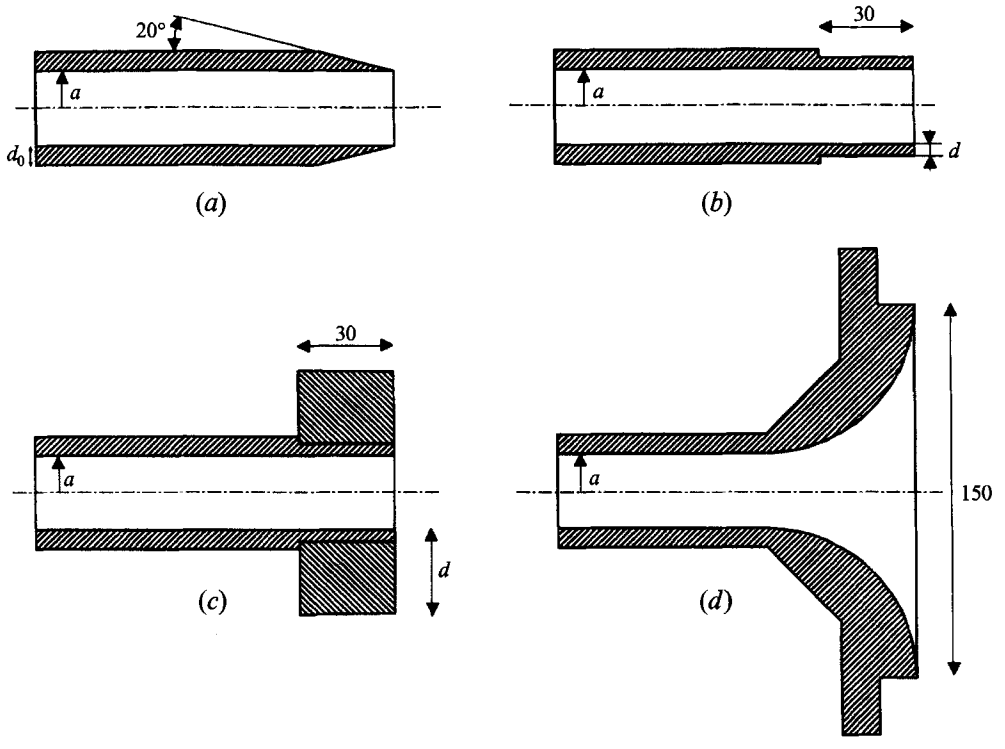

FIGURE 1. Pipe end geometries used for the experiments (dimensions in mm): (*a*) sharp-edged pipe end; (*b*) thick-walled pipe end with wall thickness d of the order of d_0; (*c*) thick-walled pipe end with wall thickness d much larger than d_0; (*d*) circular horn with radius of curvature $r = 4a$.

2. Set-up and experimental procedure

2.1. *Set-up*

The measurements have been carried out in a horizontal steel tube of 6 m length and inner radius $a = 15.013$ mm. The wall thickness of the tube is $d_0 = 5.00$ mm. The inner pipe wall has a surface roughness of less than 0.1 μm, which in all the applications considered here corresponds to an hydraulically smooth surface. A very thin coating of oil was present in order to avoid possible corrosion of the tube. The experimentally determined friction coefficient agreed within the accuracy of the volume flow measurement (0.5%) with the one that follows from Prandtl's law for the friction of a tube with hydraulically smooth walls (Schlichting 1968).

The open pipe end is placed in the middle of a large room ($20 \times 16 \times 9$ m^3), 0.66 m above a rigid floor. The nearest wall is at 6 m distance. The four different types of pipe end geometries studied in this paper are given in figure 1. The first, shown in figure 1(*a*) and approximating the unflanged pipe termination with thin walls studied by Levine & Schwinger (1948), Munt (1977, 1990) and others, has a sharp edge with a bevel angle of 20°. The second type of geometry, given in figure 1(*b*), is an unflanged pipe end with thick walls, with thickness d comparable with the thickness d_0 of the pipe wall. Two values of the wall thickness d at the pipe end were chosen, with for ratios of inner to outer radius $a/(a+d) = 0.85$ and 0.70, each corresponding with geometries studied by Ando (1969). Experiments with pipe end wall thicknesses d larger than the pipe radius a, i.e. $d/a = 4/3$ and $20/3$, i.e. with the type of pipe end geometry given in figure 1(*c*), were carried out to obtain values for the end correction for conditions close to those

of a flanged pipe end. Finally a pipe end with a circular horn with radius of curvature r equal to $4a$, shown in figure 1(*d*), was studied. This geometry is a reasonable approximation for the human lips when whistling.

In the absence of a mean flow, the acoustic excitation is provided by a loudspeaker enclosed in a box with a hole of radius a at both sides of the box. One of the holes is placed at a distance 1 mm from the pipe entrance. By closing the remaining gap with flexible tape, the possible influence of acoustical streaming on the high-amplitude measurements was checked. No significant influence was observed. Mechanical contact between the pipe and the excitation is avoided by placing these elements on two independent frames. To avoid the transfer of mechanical vibrations from the loudspeaker to the pipe via the floor, the frame supporting the pipe is placed on six rubber strips. In order to obtain an optimal signal-to-noise ratio, the measurements were performed at frequencies corresponding to acoustic resonances of the pipe/excitation combination. Measurements of the reflection coefficient at a closed pipe have confirmed that there is no significant effect of pipe wall vibrations on the results of the measurements.

In the presence of a mean flow, the acoustic pulsations are provided by a siren (see figure 2*a*) which is, in the frequency range considered ($10 < f < 1000$ Hz), a much more efficient sound source than the loudspeaker. A bypass allows a variation of the ratio of the amplitude of the acoustic velocity $\hat{u}_{ac}$ at the open pipe end and the mean flow velocity U_0 in the range $0.01 < \hat{u}_{ac}/U_0 < 0.5$. When the siren and the pipe are detached to allow the mean flow to escape through the gap between the two devices, the siren can be used to excite a pipe with a closed end. This allows the comparison of the reflection coefficient at a closed pipe end obtained by excitation with the loudspeaker with that obtained with the siren. High-amplitude acoustic fields could easily be obtained using the siren as a sound source, which however can induce significant temperature variations along the pipe. The present investigation is limited to low and intermediate values of the acoustic amplitude. When the siren was rigidly attached to the pipe, with an open side branch to deflect the mean flow, a small but significant deviation of the reflection coefficient of the closed pipe end was found (0.5 %) for those frequencies, corresponding to the mechanical resonance frequencies of the set-up. With a gap of about 1 cm between the siren and the pipe end, the mechanical contact was avoided and the effect of the mechanical vibration on the reflection coefficient became negligible. Since the measurements for a closed pipe end are much more sensitive to small errors than measurements for an open pipe end, this implies that the siren does not induce significant vibrations in the pipe walls. However, in order to ensure that wall vibrations do not affect the data, the siren and the pipe were detached and the gap was closed with flexible plastic tape.

The speed of sound c_0 is calculated from the wall temperature T_w measured at various positions in the pipe. The variation of the temperature along the tube is about 0.1 °C, which corresponds with the uncertainty in its measurement. Using a 0.2 mm thermocouple placed across the tube, it was verified that the stagnation temperature of the flow did not differ by more than 0.2 °C from the wall temperature under the conditions considered ($M < 0.1$). The flow temperature T was calculated by assuming a recovery factor $T = T_w(1-0.18M^2)$ corresponding to a turbulent boundary layer at a plane surface according to Ronneberger (1975). The speed of sound was estimated by interpolation of the data found in Weast (1976). For measurements without a mean flow the speed of sound c_0 is corrected for the humidity of the air. For the experiments with mean flow the air is provided by a high-pressure supply (60 bar) and is dry (dewpoint −40 °C).

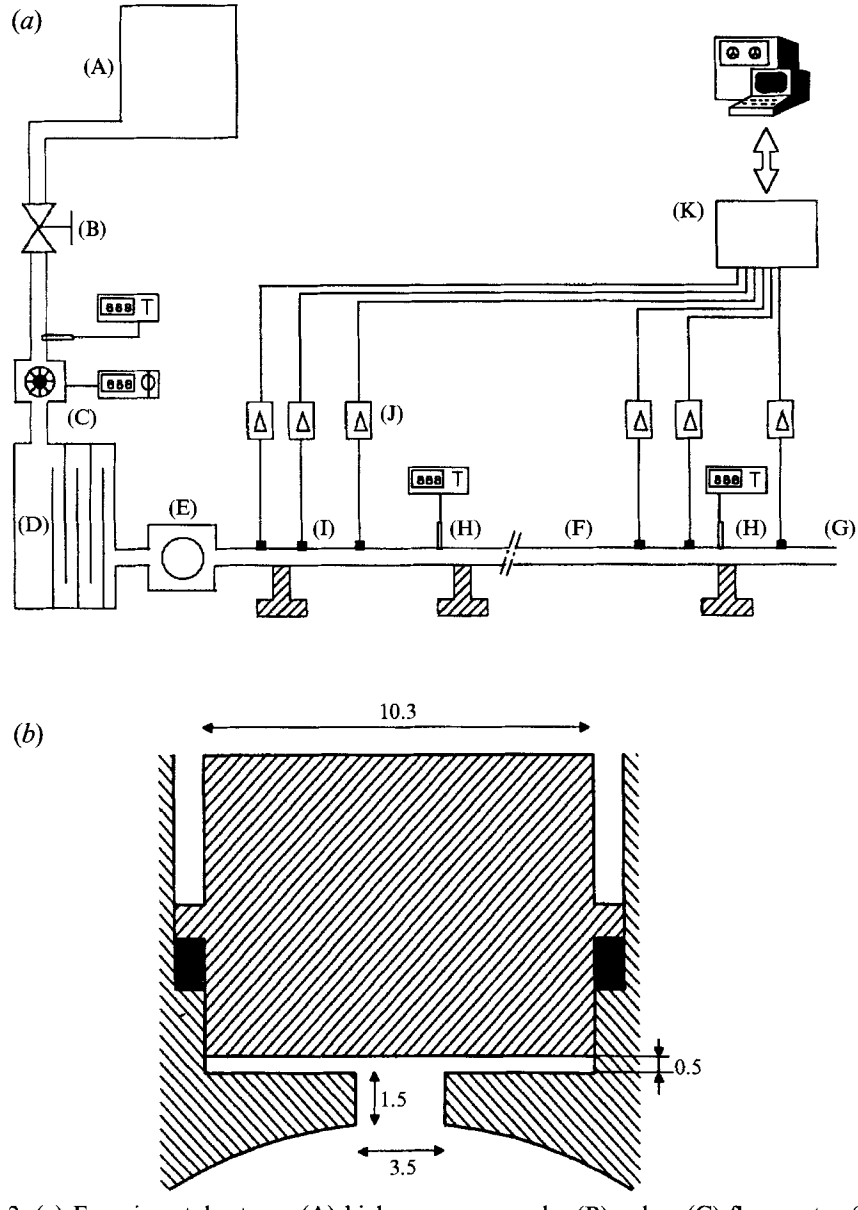

FIGURE 2. (*a*) Experimental set-up: (A) high-pressure supply, (B) valve, (C) flow meter (Instomet Q-66), (D) reverberation chamber, (E) siren, (F) steel tube (inner radius $a = 0.015\,013$ m), (G) pipe end geometry, (H) wall temperature measurement, (I) pressure transducers (type PCB 116 A), (J) charge amplifiers (type Kistler 5007), (K) data acquisition system (HP 3656 S). (*b*) Configuration of the pressure gauges in the pipe wall (dimensions in mm).

The mean flow velocity U_0 is calculated from the volume flow obtained with a calibrated turbine meter (type Instromet Q-66). The uncertainty in the measurement of U_0 is about 0.5%. The measured U_0 is corrected for the difference in pressure and temperature between the pipe exit and the flow meter position. The calibration of the turbine meter was checked by a comparison of the measured mean velocity with the value obtained from the profile for a fully developed turbulent pipe flow where the centreline velocity was measured by a Prandtl tube. Also, a comparison with data

obtained with an orifice meter showed that the measured mean velocity is accurate to within 0.5%.

The mean static pressure in the pipe was measured using a Wallace & Tiernan manometer with a measurement accuracy of 50 Pa. The atmospheric pressure was determined with a mercury manometer with an error of less than 100 Pa. The acoustic pressure in the pipe is measured by means of acceleration-compensated piezo-electrical gauges (type PCB 116 A). These gauges have a diameter of 10.3 mm. Because the diameter of the gauges is large compared to the pipe radius, the gauges cannot be mounted flush in the pipe wall. The installation of the gauges in the wall of the pipe is shown in figure 2(*b*). A channel (3.5 mm diameter and 1.5 mm long) connects the pipe with a cylindrical cavity (10.5 mm diameter and 0.5 mm deep) in front of the surface of the pressure gauge. Calibration of the installed gauge involving a reference pressure gauge mounted flush in a closed pipe end yields a correction on the gauge readings for the influence of the gauge installation units.

The pipe consists of separate segments on which the individual pressure gauges are mounted. By interchanging these pipe segments, different positions of the microphones are obtained. As will be shown in the next section, the accuracy of the data depends on the relative position of the gauge with reference to the standing wave pattern in the pipe and hence on the frequency considered. As a rule of thumb, one of the gauges used for the determination of the reflection coefficient must be placed close to a pressure node. In the case of an open pipe end the first microphone is placed about three diameters from the pressure node at the pipe end. At this position a plane wave approximation yields an accurate description of the acoustical field. The proximity of this first microphone to the pressure node at the open pipe end implies that measurements will be accurate for a continuous range of frequencies. One of the microphones has to be positioned at a pressure node, which implies that when a closed pipe end is considered, or when data obtained at a location further down the pipe are considered (for example for the measurement of damping), full accuracy of the data is only achieved for discrete frequencies.

The position x_i, measured from the pipe end, of microphone i was determined with an accuracy of 0.1 mm. Measurements for a closed pipe end confirm that the acoustical position of the gauge corresponds with the geometrically determined position of the gauge. The signals from the microphones are amplified by means of charge amplifiers (Kistler type 5007, bandwidth $0.1\ \text{Hz} < f < 22\ \text{kHz}$) and transferred for further analysis to an HP 3565S data acquisition system (dynamic range 80 dB, phase accuracy 0.1°, linearity 0.1 dB). Using FFT analysis (frequency discretization 0.004 Hz, using a Hanning window), the transfer functions H_{ij} between microphones at positions x_i and x_j were obtained. Only data with a coherence equal to 1 within the accuracy of the measurement (10^{-4}) were used. Each measurement was repeated three times.

The reproducibility of the measurements appears to be determined by the analog/digital converter (13 bit). The accuracy of the measurements is mainly limited by the accuracy of the calibration of the pressure gauges. Because the measurement for the case of the closed pipe end is very sensitive to small errors in the calibration, these measurements were used to adjust the calibration obtained with the procedure described above. With this refinement the damping coefficient in a quiescent fluid obtained from the measurement data was used, which was close to the value predicted by Kirchhoff (1868).

Because the measurements were carried out simultaneously reading up to six microphones, independent reflection coefficient data could be obtained. Data were checked for their sensitivity to systematic errors due to the uncertainties in the

calibration. Suspect data, showing errors more than 0.5% as a result of the uncertainties in the calibration, were rejected. In general, data obtained with different microphone pairs agreed to within 0.1%. Typical reproducibility of the data is of the order of 0.05% or better. The largest systematic errors observed are due to the room acoustics and will be discussed further.

2.2. *Mean flow conditions*

As the test section of the pipe was always placed more than 100 pipe diameters downstream of the siren, a fully developed turbulent mean flow was achieved in all experiments. The mean velocity profile close to the pipe end was measured by means of a constant-temperature hot wire of 5 μm diameter and 6 mm length. The average velocity U_0 inside the pipe was approximately 41 m/s, which is close to the maximum velocity used in all experiments. The measured velocity profiles in the shear layer of the free jet at a flanged pipe end are presented in figure 3. The momentum thickness of the shear layer increases linearly with the distance to the pipe end. For the steady flow in a pipe segment ended by a horn, the separation point depends strongly on the Reynolds number for the flow conditions considered. This effect is measured by means of a pressure recovery factor, defined by $C_D = \Delta p/\frac{1}{2}\rho_0 U_0^2$, where Δp is the pressure difference between a point inside the pipe in front of the horn and a point in the far field outside. This pressure recovery factor is presented in figure 4 and can be related to an effective diameter D_j of the free jet, assuming a uniform free jet flow and using the Bernoulli equation, by $C_D = 1-(2a/D_j)^4$. The maximum pressure recovery factor is $C_D = 0.3$, which is equivalent to a maximum increase of the jet width of about 10%.

2.3. *Determination of reflection coefficient and damping*

Using the measured transfer functions H_{ji} between the microphone at position x_j and the reference microphone at position x_i, close to the open pipe end ($x = 0$), the reflection coefficient R of the open pipe end and the complex-valued wavenumbers k_+ and k_- of the acoustic waves travelling in positive and negative directions, can be determined. The underlying analysis is based on the assumption that the acoustic field can be described in terms of plane waves for which $p(x,t) = \hat{p}(x)\,\mathrm{e}^{\mathrm{i}\omega t}$ with

$$\hat{p}(x) = \hat{p}_+\,\mathrm{e}^{-\mathrm{i}k_+x} + \hat{p}_-\,\mathrm{e}^{\mathrm{i}k_-x}, \tag{1}$$

where $\hat{p}$ is the complex-valued amplitude of the acoustic pressure $\hat{p}(x)$ and ω is radian frequency. The imaginary parts of the wavenumbers $\mathrm{Im}(k_\pm)$ correspond to the negative of the damping coefficients $\alpha_\pm$ of the waves,

$$\alpha_\pm = -\mathrm{Im}(k_\pm). \tag{2}$$

When the wavenumbers $k_\pm$ and the transfer function $H_{ji} = \hat{p}(x_j)/\hat{p}(x_i)$ are known, the complex-valued reflection coefficient $R(x)$ at position x, defined as

$$R(x) = \hat{p}_-\,\mathrm{e}^{\mathrm{i}k_-x}/\hat{p}_+\,\mathrm{e}^{-\mathrm{i}k_+x} \tag{3}$$

can be calculated from

$$R(x) = \frac{H_{ji}\,\mathrm{e}^{-\mathrm{i}k_+(x_i-x)} - \mathrm{e}^{-\mathrm{i}k_+(x_j-x)}}{\mathrm{e}^{\mathrm{i}k_-(x_j-x)} - H_{ji}\,\mathrm{e}^{\mathrm{i}k_-(x_i-x)}}, \tag{4}$$

where $k_\pm$ is assumed to be independent of the position x. If the wavenumbers $k_\pm$ are known, the reflection coefficient can be determined by the two-microphone method described by Boden & Abom (1986). The reflection coefficient at the pipe end $R(0)$ will be denoted R. If the wavenumbers $k_\pm$ are unknown as well, a multi-

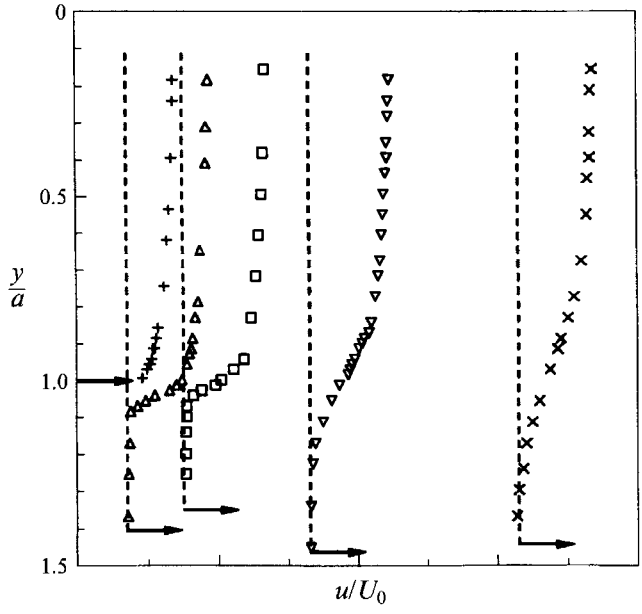

FIGURE 3. Velocity profile measured close to a flanged circular pipe end. The arrow denotes the mean velocity in the pipe (41 m/s). Measurements presented are obtained at various distances from the pipe end: +, $x = -0.2a$; △, $x = 0.15a$; □, $x = 0.7a$; ▽, $x = 1.9a$; ×, $x = 3.9a$.

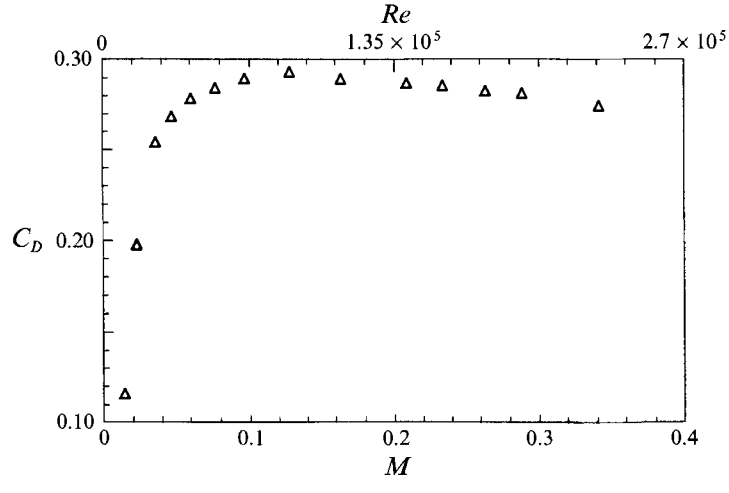

FIGURE 4. Pressure recovery factor for the steady flow in the horn shown in figure 1(*d*).

microphone method can be used. When four microphones are used, three independent pairs of microphones can be selected. From (4) a set of three nonlinear equations is obtained with R, k_+ and k_- as complex-valued unknowns. When more than four microphones are used, a nonlinear regression procedure can be used to solve the resulting set of overdetermined nonlinear equations (e.g. Ronneberger & Ahrens 1977). The procedure used for the experiments presented in this paper is based on the concentration of microphones into *two clusters*. The first cluster of microphones is placed near the pipe end. The second cluster is placed at a distance from the open pipe

end which is much larger than the microphone spacing within a cluster. The first cluster is used to determine the reflection coefficient $R(x_i)$ at position x_i of the microphone closest to the pipe end. The second cluster is used to calculate the reflection coefficient $R(x_j)$ at position x_j of the microphone of the second cluster placed in *a pressure node*. (This last condition determines the values of frequencies at which the experiments are carried out.) Under these conditions $R(x_i)$ and $R(x_j)$ appear to be most insensitive to random errors, calibration errors and other systematic errors. It was found that the values of $R(x_i)$ and $R(x_j)$ calculated using (4) for both clusters is rather insensitive to the precise value of $k_\pm$ as long as the microphones in each cluster are placed within a quarter of the acoustic wavelength. When a theoretical value is used for $k_\pm$, an accurate first approximation for $R(x_i)$ and $R(x_j)$ can be obtained. From these values of the reflection coefficient, an accurate first guess for the damping coefficient $\alpha_\pm$ can be determined from the imaginary part of the individual complex values of k_+ and k_- obtained from

$$e^{-ik_+\Delta x_{ij}} = H_{ij}\left(\frac{1+R(x_j)}{1+R(x_i)}\right), \tag{5}$$

$$e^{ik_-\Delta x_{ij}} = H_{ij}\left(\frac{1+R(x_j)}{1+R(x_i)}\right)\frac{R(x_i)}{R(x_j)}, \tag{6}$$

where $\Delta x_{ij} = x_i - x_j$ is the distance between the microphones at the position x_i and x_j. In principle, because there is a mean pressure gradient along the pipe, the Mach number M and wavenumbers $k_\pm$ depend on the position x. Using the correction procedure by Ronneberger & Ahrens (1977) this effect was estimated, but it appeared to be negligible for our experimental conditions ($M \leqslant 0.1$). Therefore here it is assumed that M and $k_\pm$ are independent of position x. The complex-valued average wavenumber $k_0 = \frac{1}{2}(k_- + k_+)$ can be obtained by averaging k_+ and k_- or directly from

$$\frac{R(x_i)}{R(x_j)} = e^{2ik_0\Delta x_{ij}}. \tag{7}$$

This procedure can either be repeated, using the new values of the wavenumbers $k_\pm$ to recalculate $R(x_i)$ and $R(x_j)$, or one can use a general nonlinear solver procedure to determine R, k_+ and k_- from the signals of two pairs of microphones (one pair in each cluster). It turned out that both procedures converged rapidly towards the same result. Typical accuracy in $|R|$ using the two-microphone method with theoretical estimates for the wavenumbers $k_\pm$ is better than 0.2% for $0.1 < ka$ and 0.3% for $0.1 < ka < 0.3$. The typical absolute accuracy in δ is about $0.03a$. For the multi-microphone method the accuracy could be increased to 0.1% for $|R|$, and to $\pm 0.02a$ uncertainty for δ. The accuracy of the wavenumber $k_\pm$ is 2% for the imaginary part and 0.02% for the real part. The reproducibility was found to better than 0.05% for $|R|$ and 0.5% for δ and $\mathrm{Im}(k_\pm)$. This accuracy was confirmed by measurements without a mean flow, and will be described in the following sections.

The energy reflection coefficient R_E is defined as the ratio of the intensities of the reflected the incident acoustic energy at the pipe end. The energy reflection coefficient R_E is related to the pressure reflection coefficient R by (Mechel 1965)

$$R_E = |R|^2\left(\frac{1-M}{1+M}\right)^2, \tag{8}$$

where $M = U_0/c_0$ is the Mach number, averaged over the duct cross-section.

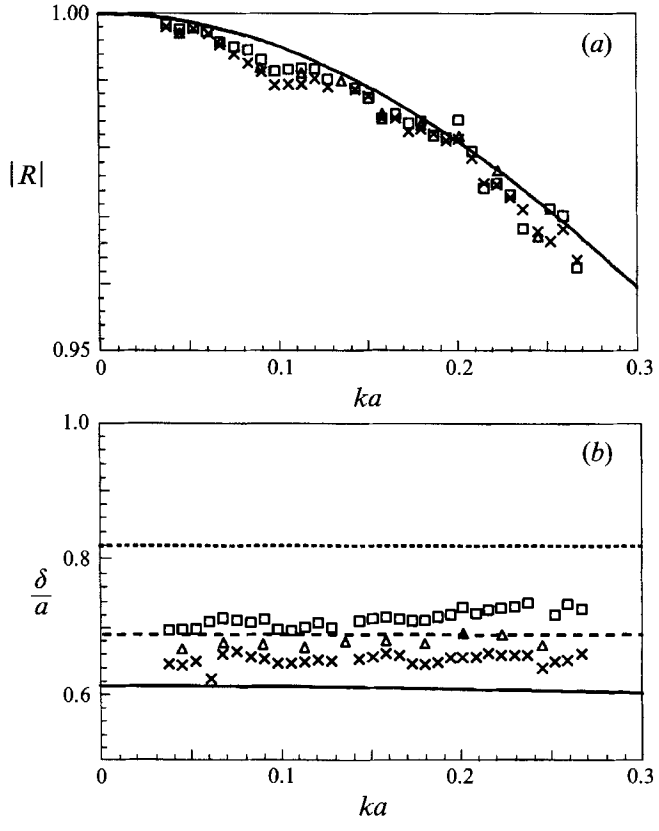

FIGURE 5. Influence of wall thickness on the reflection coefficient for an open pipe end without a mean flow at low acoustic amplitudes ($Sr_{ac} > 20$) as a function of the Helmholtz number ka. Influence of room resonances is observed mainly for $ka \approx 0.1$. A two-microphone method, using an experimentally determined value of the damping α_0, close to the value given by (11) is used. Microphone positions: $x_1 = -86.8$ mm, $x_2 = -224.5$ mm. ×, Sharp edges, $a/(a+d) = 1.00$. Thick walls: Δ, $a/(a+d) = 0.85$; □, $a/(a+d) = 0.70$. (*a*) Absolute value of the reflection coefficient $|R|$; (*b*) end correction δ: ——, Levine & Schwinger (1948) for $a/(a+d) = 1.00$ and Ando (1969) for $a/(a+d) = 0.85$. In (*b*): – – –, Ando, (1969) for $a/(a+d) = 0.70$; ....., Nomura *et al.* (1960) for $a/(a+d) = 0$.

2.4. *Influence of the acoustics of the room*

The influence of the rigid floor on the reflection coefficient of the open pipe end is taken into account by assuming a point source below the floor, at the mirror-imaged location of the pipe end, of strength equal to the acoustic volume flow at the pipe end. This image source represents the reflection of the acoustic field at the floor. Free field conditions are assumed above the floor, i.e. reflections at the ceiling and the side walls are not taken into account. As the nearest wall is at 6 m, direct reflections at this wall are negligible. The correction to the reflection coefficient and end correction due to the presence of the floor is in the low-frequency approximation given by (Disselhorst & van Wijngaarden 1980)

$$|R_{fl}| - |R| = -\frac{(ka)^2}{4kH}\sin(2kH), \tag{9}$$

$$\delta_{fl} - \delta = \frac{a^2}{8H}\cos(2kH), \tag{10}$$

where H is the distance of the pipe to the floor and $|R_{fl}|$ and δ_{fl} are the reflection coefficient and end correction in the presence of the floor, respectively. $|R|$ and δ are the values for the latter two quantities for free field conditions. For low Helmholtz numbers, i.e. $ka < 0.3$, the correction in our experiments (with $H = 660$ mm and $a = 15.013$ mm) is less than 0.2% for an open pipe end. Nevertheless it has been applied to all data presented here.

Figure 5 compares the reflection coefficient $|R|$ and end correction δ obtained with a two-microphone method, in the absence of a mean flow, with the theoretical results of Levine & Schwinger (1948) for an unflanged pipe end with thin walls, and the theory of Ando (1969) for pipes with finite wall thickness d. It is found that the data for $|R|$ obtained from the present measurements agree within 0.5% with the theoretical data, while the data for δ obtained from the experiments agree within 5% with the theoretical data. The data presented in figure 5 are obtained for low values of the acoustic displacement compared to the pipe radius. This condition can be expressed in terms of an acoustic Strouhal number $Sr_{ac} = \omega a/\hat{u}_{ac}$. The data of figure 5 are obtained for conditions such that $Sr_{ac} > 20$. For acoustic Strouhal numbers in this range there is no significant nonlinear behaviour to be expected.

The main systematic difference between the reflection coefficient obtained from the measured and the theoretical data occurs around $ka = 0.1$. It is expected that this apparent systematic error of about 0.5% is due to the resonance of the large room in which the experiments have been carried out.

3. Damping

In §§3.1–3.3, the existing theories and data on damping of plane waves in smooth pipes will be discussed. New data obtained with the multi-microphone method described in the previous section are presented in §3.4.

3.1. *Damping in the absence of mean flow*

Viscothermal damping of acoustic waves in a quiescent medium in pipes has been studied by Kirchoff (1868), Rayleigh (1896, pp. 319–326) and Tijdeman (1975). In the low-frequency approximation, for which $ka \ll 1$ and for high shear numbers $Sh = a(\omega/\nu)^{\frac{1}{2}} \gg 1$, where ν is the kinematic viscosity of the medium, the wavenumber can be approximated by

$$k = \frac{\omega}{c_0}\left(1 + \frac{1-\mathrm{i}}{\sqrt{2}}\frac{1}{Sh}\left(1 + \frac{\gamma-1}{Pr^{\frac{1}{2}}}\right) - \frac{\mathrm{i}}{Sh^2}\left(1 + \frac{\gamma-1}{Pr^{\frac{1}{2}}} - \tfrac{1}{2}\gamma\frac{\gamma-1}{Pr}\right)\right), \tag{11}$$

where γ and Pr are the ratio of the specific heats, also known as Poisson's ratio, and the Prandtl number, respectively. In the experiments described in this paper $ka < 0.3$ while $Sh > 20$. For air $Pr = 0.71$ and $\gamma = 1.4$. The density ρ_0 of air was taken from Weast (1976). For the dynamic viscosity of air $\eta = \rho\nu$ the data given by Touloukian, Saxena & Hestermans (1975) were used. As a result, the temperature dependence of the kinematic viscosity of dry air is given by $\nu = A + B(T - T_{ref})$, with T the absolute temperature of the air inside the pipe, $A = 1.51\ 10^{-5}$ m^2/s, $B = 9.2 \times 10^{-8}$ m^2/sK and $T_{ref} = 293.16$ K. The first correction to ω/c_0, which is inversely proportional to the shear number, corresponds to the solution given by Kirchhoff (1868), and it also changes the phase velocity of the acoustic plane waves. The second term, i.e. the Sh^{-2} term, is a correction of the damping obtained by Kirchhoff (1868) and was obtained by Ronneberger (1975) from the exact expression given in Tijdeman (1975). The result

for $Sh > 20$ is, to within 0.01 %, in agreement with the low-frequency solution obtained by Tijdeman (1975).

The damping in a quiescent fluid is given by the negative of the imaginary part of (11), i.e.

$$\alpha_0 = \frac{\omega}{c_0}\left(\frac{1}{\sqrt{2}\,Sh}\left(1+\frac{\gamma-1}{Pr^{\frac{1}{2}}}\right)+\frac{1}{Sh^2}\left(1+\frac{\gamma-1}{Pr^{\frac{1}{2}}}-\tfrac{1}{2}\gamma\frac{\gamma-1}{Pr}\right)\right). \tag{12}$$

Although the Sh^{-2} term in (12) is usually neglected in the literature (e.g. Davies 1988; Morse & Ingard 1968; Pierce 1989) in our experiments it can attain values of 2% of the first term. Hence this correction should be taken into account in view of the experimental accuracy (1%) which is to be achieved in the damping.

The dissipation is dominated by the viscothermal losses at the walls. The viscothermal losses in the bulk of the flow are given by Pierce (1989) as

$$\alpha_{bulk} = \frac{\omega}{c_0}\frac{(ka)^2}{2Sh^2}\left(\frac{4}{3}+\frac{\mu_B}{\mu}+\frac{\gamma-1}{Pr}\right), \tag{13}$$

where μ_B is the bulk viscosity which is approximately 0.6μ. The contributions due to relaxation processes can be accounted for by an enhanced bulk viscosity (Pierce 1989, chap. 10), which for low frequencies dominates the other contributions given in (13). This contribution to the damping is two orders of magnitude smaller than the losses in the boundary layer and will be neglected.

3.2. *Convective effects*

The wavenumbers for up- and downstream propagating acoustic waves are influenced by the mean flow velocity U_0, defined as the volume flux divided by the ripe cross-section. For a uniform mean flow, neglecting damping, it is found that

$$k_\pm = \frac{\omega/c_0}{1\pm M}, \tag{14}$$

where $M = U_0/c_0$ is the Mach number of the mean flow. The effect of a non-uniform laminar mean velocity distribution on the damping coefficient was studied by Ronneberger (1975). By taking into account the turbulent mean velocity profile Ronneberger (1975) solved the linearized equations for mass, momentum and energy conservation for a pipe flow. In this quasi-laminar theory the acoustic effect of the turbulent mixing was neglected. When the acoustic boundary-layer thickness $\delta_{ac} = (2\nu/\omega)^{\frac{1}{2}}$ is small compared to the viscous sublayer $\delta_l \approx 10\nu/v^*$ of a turbulent pipe flow (where $v^* = (\tau_0/\rho_0)^{\frac{1}{2}}$ is the friction velocity), the quasi-laminar theory is expected to describe the damping of the acoustic waves quite accurately. To a first-order approximation, the damping coefficient is independent of the mean flow velocity distribution, but dependent only on the mean flow Mach number according to (Ronneberger 1975)

$$\frac{\alpha_-}{\alpha_+} = \left(\frac{1+M}{1-M}\right)^2\frac{[1/(1-M)^2]+(\gamma-1)/Pr^{\frac{1}{2}}}{[1/(1+M)^2]+(\gamma-1)/Pr^{\frac{1}{2}}}, \tag{15}$$

valid for the region where $\delta_{ac} < \delta_l$. Using a two-dimensional flow model, Howe (1984) found an alternative result which for $\delta_{ac} < \delta_l$ is given by

$$\frac{\alpha_-}{\alpha_+} = \frac{[1/(1-M)^2]+(\gamma-1)/Pr^{\frac{1}{2}}}{[1/(1+M)^2]+(\gamma-1)/Pr^{\frac{1}{2}}}. \tag{16}$$

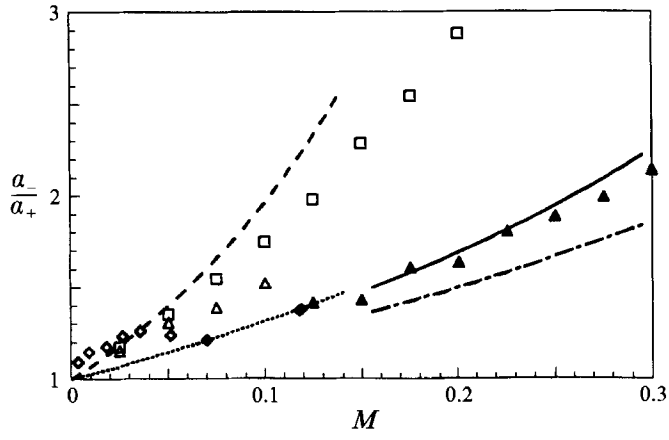

FIGURE 6. Influence of Mach number of the damping coefficient in the upstream (α_-) and downstream (α_+) directions. △, $f = 630$ Hz; □, $f = 3350$ Hz: data of Ronneberger & Ahrens (1977). (◇), $f = 135$ Hz: data obtained with a multi-microphone method with microphones at positions $x_1 = -86.8$ mm, $x_2 = -347.8$ mm, $x_3 = -385.3$ mm, $x_4 = -4550.3$ mm, $x_5 = 4601.2$ mm, $x_6 = -5093.7$ mm. Data corresponding to values for which $\delta_{ac}/\delta_l > 1$ are shown as solid symbols. Theory for $\delta_{ac}/\delta_l \ll 1$: -----, quasi-laminar theory, Ronneberger (1975), equation (15); ....., Howe (1984), equation (16); and for $\delta_{ac}/\delta_l \gg 1$: –·–·–, Ingard & Singhal (1974), equation (18); ——, Howe (1984), equation (19).

Since the theory of Howe (1984) is a cruder approximation than the one used by Ronneberger (1975), we expect the result given by Ronneberger (1975) to be more accurate for $\delta_{ac} < \delta_l$. In figure 6 the data of Ronneberger & Ahrens (1977) for the damping coefficients are given as a function of the Mach number. The data were obtained by varying the Mach number keeping the frequency constant (630 Hz (△) and 3350 Hz (□)). For the region where $\delta_{ac}/\delta_l < 1$ the data are given by open symbols, while data for $\delta_{ac}/\delta_l > 1$ are given as solid symbols. Included in figure 6 are the two theoretical results given by (15) and (16). For $\delta_{ac}/\delta_l < 1$, the quasi-laminar theory of Ronneberger (1975) describes the convective effects quite accurately. However, for the region where the turbulence affects the acoustic damping $\delta_{ac}/\delta_l \gg 1$, a strong deviation from the theory of Ronneberger (1975) is observed. Note, that (15) is only a first approximation of the quasi-laminar theory of Ronneberger (1975). Comparison with the full quasi-laminar solution can be found in Ronneberger & Ahrens (1977). The effect of turbulence on the acoustic damping properties will be described in the next subsection.

3.3. *Influence of turbulence*

In the presence of a turbulent mean flow, the damping of acoustic waves is influenced by the action of the turbulent stresses, if the acoustic boundary-layer thickness δ_{ac} is larger than the laminar sublayer δ_l. The effect of turbulence can be described to a first-order approximation by adding to the kinematic viscosity an eddy viscosity, which is non-uniform over the pipe cross-section. The eddy viscosity is small compared to the kinematic viscosity for distances from the wall (y) small compared to the thickness of the viscous sublayer δ_l. For $y > \delta_l$, in the logarithmic region of the turbulent boundary layer, the eddy viscosity increases approximately linearly with the distance from the wall. Using van Driest's hypothesis (see Schlichting 1968) for the calculation of the eddy viscosity, Ronneberger & Ahrens (1977) derived a model for the damping of acoustic waves by a turbulent mean flow. From their experimental data three different regions could be distinguished in terms of the relative thickness of the acoustic

boundary layer. For low values of the ratio δ_{ac}/δ_l, the damping of acoustic waves is not influenced by the turbulent shear stress and is accurately described by the quasi-laminar theory of Ronneberger (1975) (figure 6). This finding fully agrees with the observation that the eddy viscosity is small in the viscous sublayer. For large values of δ_{ac}/δ_l, the damping was found to increase linearly with the acoustic boundary-layer thickness. In this case, the damping is mainly a result of the turbulent mixing in the bulk of the flow. For a value of the ratio δ_{ac}/δ_l of order one, at a critical Mach number a minimum in the damping was observed by Ronneberger & Ahrens (1977). This minimum is lower than the value predicted by the quasi-laminar theory. Hence Ronneberger & Ahrens (1977) conclude that the damping appears to be reduced by the presence of turbulence. They explain this to be a result of the destructive interference at the wall of the shear waves generated by the acoustic field with the shear waves reflected at the edge of the viscous sublayer by the strong variation of the eddy viscosity. For critical ratios of the acoustic boundary-layer thickness and the thickness of the laminar sublayer, this destructive interference is maximal which results in the observed minimum in the damping.

Using the eddy viscosity model of van Driest (Schlichting 1968), Ronneberger & Ahrens (1977) could not predict the minimum in the damping. In their model the damping coefficient $\alpha_0 = \lim_{M\to 0} \alpha_\pm$ was always larger than the damping in the absence of a turbulent mean flow.

Using a model for the eddy viscosity in which the eddy viscosity depends linearly on the distance from the wall and in which the eddy viscosity is neglected within the viscous sublayer, Howe (1984) did predict a minimum of the damping coefficient α_0. However, the minimum in α_0 does not appear at the correct value of δ_{ac}/δ_l, and the interference effect is severely underestimated.

Even the simplified 'rigid plate' model, proposed by Ronneberger & Ahrens (1977), assuming an infinitely large eddy viscosity, which certainly overestimates the reflection of the shear wave at the edge of the viscous layer does not predict the correct δ_{ac}/δ_l at which the minimum in the damping occurs, nor the correct value of the minimum itself. Using the thickness of the laminar sublayer δ_l as a parameter to shift the position of the minimum to the observed value of δ_{ac} at minimum, the minimum in the damping is underestimated by a factor of two.

Because the shear wave decays rapidly with the distance from the wall, a deep minimum suggests reflections from a distance (y) smaller than the value of δ_l used in the existing theories. To obtain a destructive interference one should then have an additional phase shift during the reflection. This phase shift might be related to the 'memory' of turbulence. Hence in spite of the fact that Ronneberger & Ahrens (1977) assume these memory effects to be negligible, a theory neglecting these effects does not explain the available experimental data.

More recently Ronneberger (1991) estimated that the timescale involved in the memory effects of turbulence is of the order of $t_m = 100\nu/v^{*2}$. This corresponds to the acoustic period if $\omega^+ = \omega\nu/v^{*2} = 2\pi/100$. This appears to be a value of the same order of magnitude as the value of ω^+ at which the damping approaches a minimum ($\omega^+ \approx 0.01$) in the experiments of Ronneberger & Ahrens (1977).

If the rigid-plate model proposed by Ronneberger & Ahrens (1977) is extended, including a phase shift of $\omega t_m = 100\omega^+$ of the reflection at the edge of the viscous sublayer ($y = \delta_l$), the shear stress at the wall τ_0 is given by

$$\frac{\tau_0}{\tau_{Stokes}} = \frac{1+\exp[-2(1+\mathrm{i})(\delta_l^+/\delta_{ac}^+)-200\mathrm{i}/\delta_{ac}^{+2}]}{1-\exp[-2(1+\mathrm{i})(\delta_l^+/\delta_{ac}^+)]}, \tag{17}$$

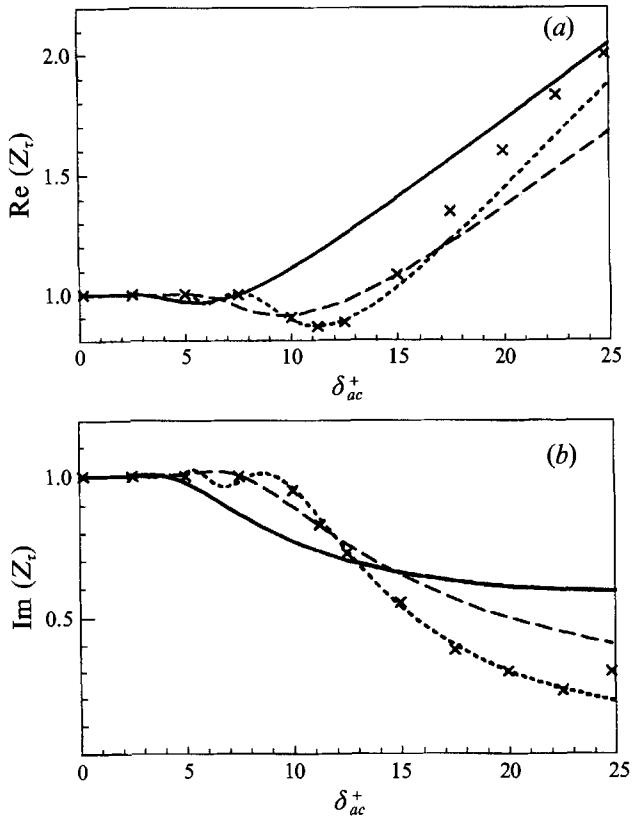

FIGURE 7. Influence of turbulence on the shear stress impedance, $Z_r = (1+\mathrm{i})\tau_0/\tau_{Stokes}$. (*a*) Real part $\mathrm{Re}(Z_r)$, (*b*) imaginary part $\mathrm{Im}(Z_r)$. ×, Experimental data of Ronneberger & Ahrens (1977). ——, rigid-plate model ($\delta_l^+ = 15$) (Ronneberger & Ahrens 1977); ....., rigid-plate model with memory effects ($\delta_l^+ = 12.5$), equation (17); ——, model (Howe 1984) ($\delta_l^+ = 7$).

where the superscript + denotes values non-dimensionalized with the kinematic viscosity ν and the friction velocity v^*, and $\tau_{Stokes} = [\mu(1+\mathrm{i})/\delta^+_{ac}]\hat{u}_{ac}\mathrm{e}^{\mathrm{i}\omega t}$ is the shear stress for a Stokes boundary layer in the absence of a mean flow. If the value of δ_l^+ is adjusted to fit the low-frequency quasi-steady limit, a value $\delta_l^+ = 12.5$ is obtained. In figure 7 the experimental data of Ronneberger & Ahrens (1977) for the wall shear stress impedance $Z_r = (1+\mathrm{i})\tau_0/\tau_{Stokes}$ in the presence of a turbulent mean flow is compared with the results of the rigid-plate model of Ronneberger & Ahrens (1977) with $\delta_l^+ = 15$, the theoretical result of Howe (1984) with $\delta_l^+ = 7$, and the modified rigid-plate model with $\delta_l^+ = 12.5$ in which a phase shift due to memory effects of turbulence is taken into account. Figure 7 clearly shows that the memory effects can be responsible for the differences between the results of existing theories and the experiments. The result given in (17), obtained by including the memory effect into the simple rigid-plate model, considerably increases the correlation between theory and the experiment. This is rather surprising, since the rigid-plate model is a very crude model of the interaction of the acoustic shear wave with the turbulent flow, away from the wall. The decrease of the wall shear stress observed by Ronneberger & Ahrens (1977) agrees with more recent data on the wall shear stress reported in Mankbadi & Liu (1992) and Louis & Isabey (1992), although the data presented there show a large scatter, in particular in the region where $\delta_{ac}/\delta_l > 1$.

For high values of the ratio δ_{ac}/δ_l the two-dimensional approximation of the boundary layer used by Howe (1979*b*, 1984) is no longer valid, because the acoustic boundary-layer thickness then becomes of the order of the radius of the pipe ($Sh \approx 1$). From the experimental data of Ronneberger & Ahrens (1977), a quasi-stationary behaviour is obtained for $\delta_{ac}/\delta_l > 2$. The two-dimensional theory of Howe (1984) does not have such a quasi-stationary limit for $\delta_{ac}/\delta_l \to \infty$ in its present form. This is a severe drawback which calls for further theoretical study.

Ingard & Singhal (1974) have derived a quasi-stationary theory for the damping in the region where δ_{ac}/δ_l is large. In their theory, the damping coefficient is given by

$$\frac{\alpha_\pm}{\alpha_k} = \frac{\delta_{ac}^+(\psi/2)^{\frac{1}{2}}}{1+(\gamma-1)/Pr^{\frac{1}{2}}} \frac{(1+\frac{1}{2}Re\,\partial \ln(\psi)/\partial Re)}{1\pm M}, \tag{18}$$

where α_k is the damping in a quiescent fluid according to Kirchhoff (1868), and is given by the first term in (12). In (18) Re is the Reynolds number, based on the mean flow velocity and the pipe diameter, and ψ is the turbulent friction factor. For smooth pipes ψ can be obtained from the Prandtl or Blasius equations (see Schlichting 1968). For high Reynolds numbers, ψ depends only weakly on the Reynolds number. The expression given by Howe (1984), can be simplified for the limit of $\delta_{ac}/\delta_l \gg 1$ to

$$\frac{\alpha_-}{\alpha_+} = \frac{[1/(1-M)^2]+(\gamma-1)/Pr}{[1/(1+M)^2]+(\gamma-1)/Pr}. \tag{19}$$

In figure 6 the convective effects in the region where $\delta_{ac}/\delta_l > 1$ can be compared with the experimental data of Ronneberger & Ahrens (1977), for a frequency of 630 Hz. In this region the theory of Howe (1984) is found to give a more accurate prediction of the convective effects than the theory of Ingard & Singhal (1974).

Ingard & Singhal (1974) obtained the frequency dependence of the damping $\alpha_\pm$ by simply adding Kirchhoff's damping α_k in the absence of flow to $\alpha_\pm$ given by (18). This is certainly a very crude approach which is not justified by existing experimental data.

A quasi-stationary limit for the damping coefficient can also be obtained from the rigid-plate model proposed by Ronneberger & Ahrens (1977) which, using the two-dimensional theory of Howe (1984), results in

$$\frac{\alpha_\pm}{\alpha_k} = \frac{\delta_{ac}^+}{\delta_l^+} \frac{[1/(1\pm M)^2]+(\gamma-1)/Pr}{1+(\gamma-1)/Pr^{\frac{1}{2}}}. \tag{20}$$

When $\delta_l^+ = 12.5$, the value of the damping is reasonably close to the result of Ingard & Singhal (1974), given by (18). However the theory of Ingard & Singhal (1974) neglects the influence of thermal convection and corresponds to an isothermal solution. The convective effects and the frequency dependence of (20) are in much better agreement with the experimental data. It should be noted however that at the moment there is no well-established theory describing the convective effects in the quasi-stationary limit.

3.4. *Experimental results*

Using the multi-microphone method the damping coefficient for plane waves travelling in a pipe in a quiescent fluid have been determined for a set-up consisting of a pipe with a closed end. The reflection coefficient of the closed pipe end is $R(0) = 1$, while a reflection coefficient $R(x_j)$ was obtained with two pairs of microphones ± 3.5 m from the closed end. From (7) the average wavenumber k_0, and as a result the damping, could be determined accurately. The damping coefficient $\bar{\alpha}$ obtained for the acoustic

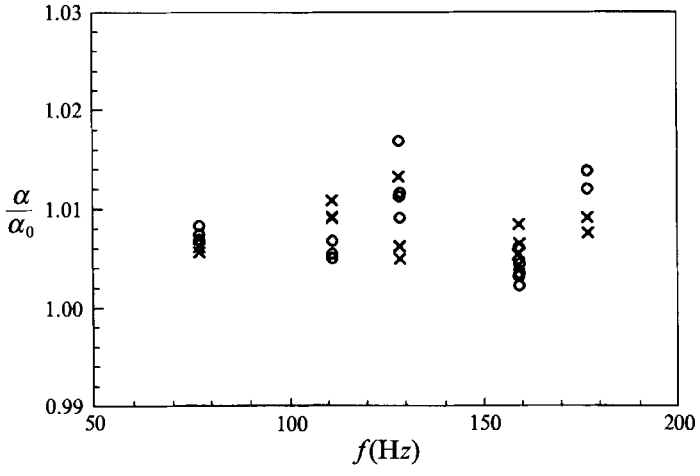

FIGURE 8. Damping coefficient in the absence of mean flow, non-dimensionalized with the value given by equation (12). A multi-microphone method is used with microphones at positions $x_1 = -7.5$ mm, $x_2 = -3426.0$ mm, $x_3 = -3476.8$ mm. ○, $(\bar{\alpha}/\alpha_0)$ obtained from $R(0) = 1$, $R(x_2)$ and H_{12}; ×, $(\bar{\alpha}/\alpha_0)$ obtained from $R(0) = 1$, $R(x_3)$ and H_{13}.

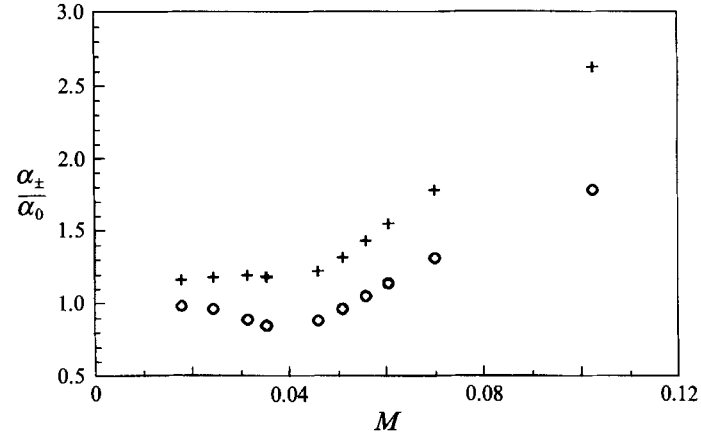

FIGURE 9. Damping coefficient $\alpha_\pm/\alpha_0$ as a function of Mach number M for constant Helmholtz number $ka = 0.0242$. Multi-microphone method with microphones at positions $x_1 = -112.5$ mm, $x_2 = -3531.0$ mm, $x_3 = -3581.8$ mm, $x_4 = -3732.0$ mm, for a pipe terminated by a sharp edge with $a/(a+d) = 1.00$. +, α_-/α_0; ○, α_+/α_0.

waves is presented in figure 8. The damping coefficient is normalized by the theoretical value for the damping α_0 in the absence of mean flow for high shear numbers (equation (12)). The data obtained with the different microphone pairs agree within the experimental accuracy ($\pm 2\%$) of $\bar{\alpha}$. Figure 8 shows that the damping is within the range of the required accuracy for the present measurements, i.e. the damping is about 0.7% larger than the value predicted by (12). This small systematic deviation can partly be explained by the viscosity in the bulk of the flow, mainly due to relaxation processes.

For the measurements without mean flow, presented in §4, the data obtained with the two-microphone method were post-processed by using the experimentally determined value of the damping.

The damping of acoustic waves in a turbulent mean flow was obtained in two ways:

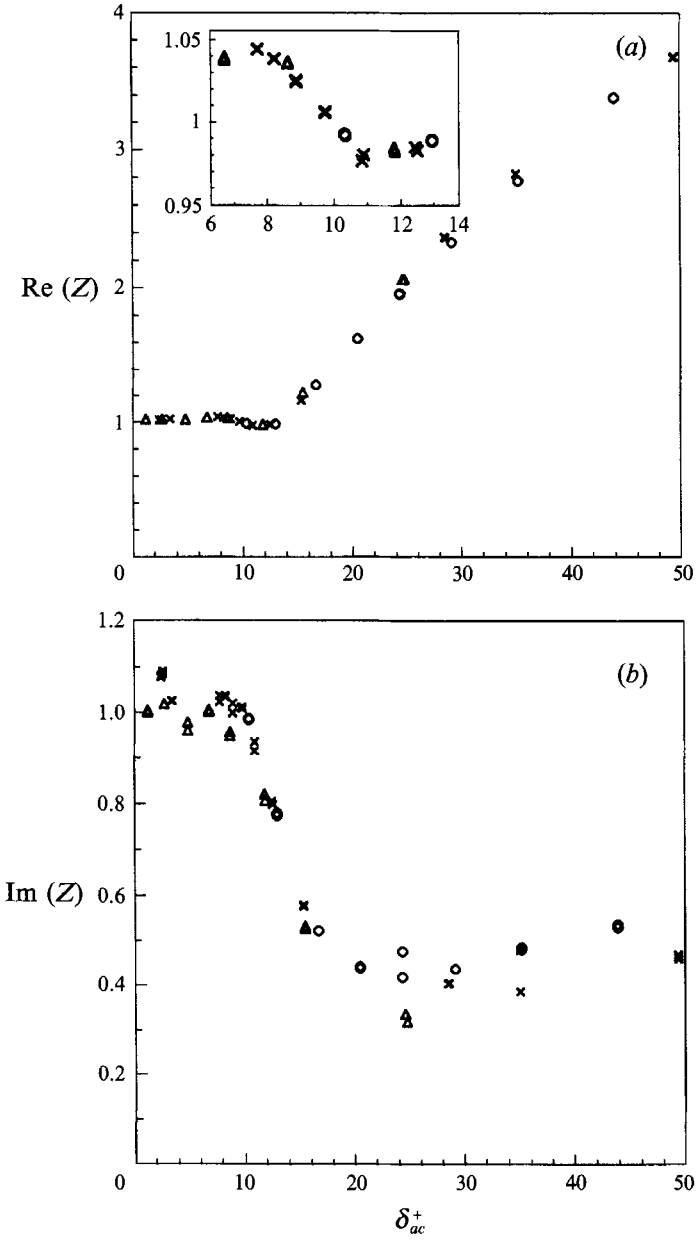

FIGURE 10. Averaged wall impedance Z obtained from the averaged wavenumber k_0. (*a*) $\mathrm{Re}(Z) = \bar{\alpha}/\alpha_0$ as a function of δ^+_{ac} with an enlargement of the region near the minimum in damping. (*b*) $\mathrm{Im}(Z) = [k_0 - (\omega/c_0)/(1-M^2)]/(-\mathrm{i}\alpha_0)$ as a function of δ^+_{ac}. Variable Mach number: △, $ka = 0.0371$; ○, $ka = 0.0121$. Variable Helmholtz number: ×, $M = 0.011$, 0.042 and 0.107.

at constant Helmholtz number by varying the Mach number, $0.01 < M < 0.1$, and at constant Mach number by varying the Helmholtz number between $0.01 < ka < 0.06$, which is the range where the microphone calibration is most accurate. In figure 9 the damping coefficients for waves travelling in the up- and downstream directions are shown as a function of the Mach number at constant frequency ($f = 88$ Hz). The damping is non-dimensionalized with the value in the absence of mean flow (equation

(12)). For high Mach numbers, a strong increase of damping is observed as the damping tends towards a quasi-stationary limit. The damping in the up- and downstream directions is different due to the presence of a mean flow.

The average wavenumber k_0 can be accurately obtained from the multi-microphone method according to (7), while the different values of the up- and downstream wavenumbers, obtained from (6), are more sensitive to calibration errors. Therefore average values, k_0, are presented in figure 10 rather then data for $k_\pm$, extrapolated to zero Mach number in the way proposed by Ronneberger & Ahrens (1977). For low Mach numbers $M < 0.1$, the difference between k_0 and $\lim_{M\to 0} k_\pm$ is of the order of M^2.

Figure 10(*a*) presents the average damping coefficient $\bar{\alpha} = \frac{1}{2}(\alpha_- + \alpha_+)$, normalized by the value in the absence of a mean flow, α_0, given in (12), as a function of δ^+_{ac}. The experimental data are again obtained in two ways: at constant frequency by varying the Mach number, and at constant Mach number by varying the frequency. Within the experimental accuracy (2% in $\mathrm{Im}(\bar{k})$) the different data sets collapse to a single curve. The data agree with the real part of the averaged wall impedance

$$Z = \lim_{M\to 0} \frac{k_0 - (\omega/c_0)/(1-M^2)}{-\mathrm{i}\alpha_0}, \tag{21}$$

which is equal to a weighted sum of the shear stress impedance Z_τ and the impedance of the heat conduction wave Z_q. In the region where $\delta_{ac}/\delta_l \approx 1$ the damping decreases significantly to a value about 3% smaller than the damping for the case without mean flow. In the region just before that ($\delta^+_{ac} \approx 7$) the damping increases slightly ($\pm 4\%$) which is clearly seen in the enlargement in figure 10(*a*). Although the data of Ronneberger & Ahrens (1977) are obtained from an extrapolation of results obtained at finite Mach number to results for zero Mach number, the difference with the average damping is less than 2% for $M < 0.1$. In the present investigation experimental data could be obtained for a value of δ^+_{ac} twice the maximum value obtained by Ronneberger & Ahrens (1977). In this region a change in the quasi-stationary behaviour is found. A similar behaviour is also observed in figure 10(*b*), which shows the imaginary part of the averaged wall impedance Z. For $\delta^+_{ac} < 25$, this parameter decreases towards a value of 0.4, which was also obtained by Ronneberger & Ahrens (1977), but a small increase is found for $\delta^+_{ac} > 25$.

The convective effect on the damping expressed in the form α_-/α_+ is given in figure 6 for a constant frequency of 135 Hz. Indeed the present low-frequency data are in reasonable agreement with the earlier data at higher frequencies (630 and 3350 Hz) of Ronneberger & Ahrens (1977), and clearly exhibit the convective effect for the different regions where $\delta_{ac}/\delta_l \gg 1$ and $\delta_{ac}/\delta_l \ll 1$.

4. Open pipe end in a quiescent fluid

4.1. *Influence of pipe end geometry*

In this section the linear behaviour of an open pipe end in a quiescent fluid is considered. The linear behaviour is found for low amplitudes of the acoustic velocity field ($\hat{u}_{ac}/c_0 \ll 1$ and $Sr_{ac} = \omega a/\hat{u}_{ac} \gg 1$).

Analytical results are in general limited to either an unflanged thin-walled open pipe in free space, or a pipe with an infinitely large hard baffle (flanged pipe end). The theory further neglects the influence of viscosity, which corresponds to the limit of high shear numbers ($Sh \gg 1$).

Because our emphasis is on low Helmholtz numbers ($ka \ll 0.3$), the acoustic field in the pipe can be described in terms of plane waves. Furthermore, in this limit the

reflection coefficient can be determined by assuming incompressible flow. At a distance r_1 from the pipe end for which $r_1/a \gg 1$ but $kr_1 \ll 1$, the flow at r_1 can be described by the incompressible flow generated by a point source. Matching the volume flow at the pipe exit with the volume flow at r_1, and mathing the acoustical energy fluxes yields the absolute values of the reflection coefficient at the pipe end, namely

$$|R| = 1 - \tfrac{1}{2}(ka)^2 \tag{22}$$

for $ka < 0.2$ for an unflanged pipe end, and

$$|R| = 1 - (ka)^2 \tag{23}$$

for $ka < 0.2$ for a flanged pipe end. The difference between these low-frequency approximations and the more accurate expressions derived by Levine & Schwinger (1948) for an unflanged thin-walled pipe end, by Ando (1969) for an unflanged thick-walled pipe end and by Nomura *et al.* (1960) for a flanged pipe end are of the order of the experimental accuracy (0.5%). In figure 5 the reflection coefficients determined from the present measurements are given for an unflanged pipe end with different values of the wall thickness ($a/(a+d) = 0.70$, 0.85 and 1.00), and compared with the exact theory of Levine & Schwinger (1948). It is indeed found from figure 5(*a*), that in the low-frequency limit the shape of the pipe end does not influence the magnitude $|R|$ of the reflection coefficient as suggested earlier by Bechert (1980).

Figure 11 shows the reflection coefficient for a pipe terminated by a horn, with a radius of curvature equal to twice the pipe diameter (see figure 1*d*). For this configuration also the theory for the unflanged pipe end appears to be valid for the magnitude of the reflection coefficient $|R|$, at least up to $ka = 0.15$ For higher frequencies, the radiation is considerably enhanced by the horn. At $ka = 0.1$ a small influence of room resonances is observed and agrees with the data for an unflanged pipe end in figure 5(*a*).

In contrast to the reflection coefficient $|R|$, the end correction δ strongly depends on the geometry of the pipe end. The end correction is a measure of the inertia of the acoustic flow around the pipe end. This effect is determined by the local flow within a region with lengthscale of the order of the pipe radius. Hence as far as $|R|$ is concerned, an unflanged pipe with a thick wall will behave like any other unflanged pipe if the wall thickness is small compared to the wavelength of the acoustic field. The end correction δ of an unflanged, thick-walled pipe is close to that of a flanged pipe end, if the wall thickness is larger than the pipe radius. Indeed, as predicted by Ando (1969) an increase of the end correction is observed from the value predicted by Levine & Schwinger (1948) for an unflanged thin-walled pipe end, i.e.

$$\delta/a = 0.6133 - 0.1168(ka)^2 \tag{24}$$

for $ka < 0.5$ towards the end correction for a flanged pipe end predicted by Nomura *et al.* (1960)

$$\delta/a = 0.8217 - 0.367(ka)^2 \tag{25}$$

for $ka < 0.5$. Figure 5(*b*) shows the end correction determined from the present measurements for an unflanged pipe end with thin ($a/(a+d) = 1.0$) and thick walls ($a/(a+d) = 0.70$, 0.85). For a pipe end with wall thickness $a/(a+d) = 0.70$, the influence of the wall thickness on the end correction observed in figure 5(*b*) agrees with the theoretical data given by Ando (1969). The theoretical data given by Ando (1969) for $a/(a+d) = 0.85$ would imply a negligible influence of the wall thickness d on the end correction δ for $ka < 0.3$. The experimental results however, show a significant increase of δ for this value of the wall thickness. As the theoretical end correction of

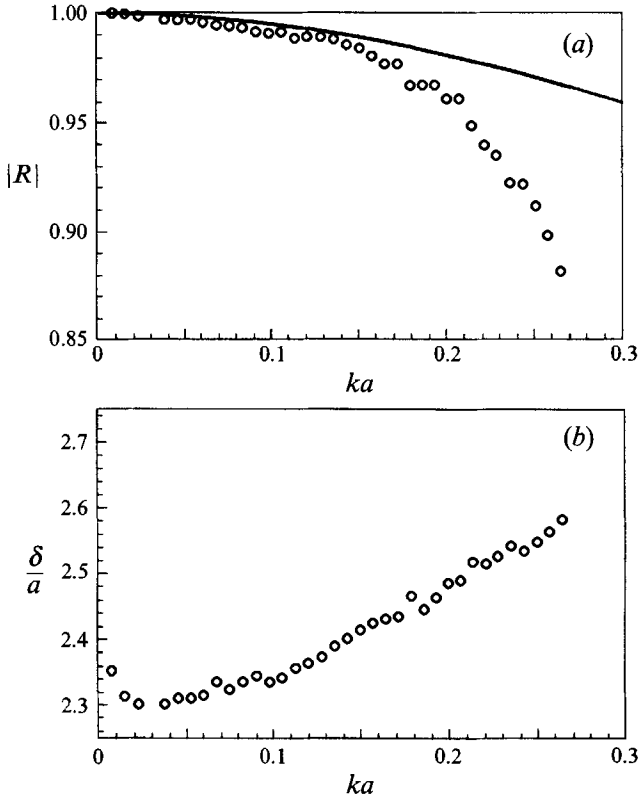

FIGURE 11. (*a*) Pressure reflection coefficient $|R|$ and (*b*) end correction δ for a pipe terminated by a horn in the absence of a mean flow as a function of the Helmholtz number ka at low acoustic amplitude. ○, Data obtained with a two-microphone method with microphones at positions $x_1 = -117.6$ mm, $x_2 = -255.3$ mm using an experimentally determined value of α_0. ——, Theory for an unflanged pipe end by Levine & Schwinger (1948).

Ando (1969) for $a/(a+d) = 0.85$ is substantially different from the experimentally determined values we think that this discrepancy is due to an error in the representation of the theoretical data, rather than a fundamental difference between the theory and experiment.

The end correction data for a pipe terminated by a horn are presented in figure 11(*b*). The end correction (defined relative to the end of the straight pipe and therefore much larger) shows a gradual increase ($\pm 13\%$) with increasing Helmholtz number ($0 < ka < 0.3$).

Using a one-dimensional approximation for the acoustic flow in the horn the end correction of the horn can be estimated to be $\delta/a = 1.92$, while a value close to 2.3 is found from the experiment. This indicates that the end correction of a horn is dominated by the inertia of the acoustic flow within the horn.

4.2. *Nonlinear losses*

The most significant nonlinear effect observed in the present experiments is the effect of the unsteady separation of the acoustic flow at the pipe end and the formation of vortices associated with the separation of the flow. This occurs when the amplitude of the acoustic displacement is large compared to the pipe radius, i.e. for conditions where the acoustic Strouhal number $Sr_{ac} = \omega a/\hat{u}_{ac}$ is small.

This nonlinear behaviour of the acoustics of a pipe end causes a strong increase in the absorption of sound since part of the acoustic energy is transferred to the kinetic energy of vortices which is subsequently dissipated by friction. The nonlinearity was studied by Bechert (1980) and Cummings & Eversman (1983) for a pipe which ends into a nozzle, and by Ingard & Ising (1967) and Cummings (1984) for a flanged pipe exit with an orifice plate at the exit. For an unflanged pipe end, without mean flow, both with sharp and with rounded edges, the nonlinear behaviour was studied extensively by Disselhorst & van Wijngaarden (1980). For high acoustic Strouhal numbers, vortices shed at the pipe end remain in the vicinity of the edges where they have been generated. Under these conditions, the vorticity generation and convection process can be described qualitatively by a locally two-dimensional potential flow model, employing for example discrete point vortices as proposed by Disselhorst & van Wijngaarden (1980). Peters & Hirschberg (1993) have shown that similar results can be obtained using a model with a single point vortex in combination with a vortex segment attached to the edge. In contrast to Disselhorst & van Wijngaarden (1980), the single vortex model predicts an acoustic energy absorption which is a factor 2.5 lower than the value observed experimentally at a sharp-edged pipe end. Comparison of the two-dimensional flow model with flow visualization of a two-dimensional flow by Disselhorst & van Wijngaarden (1980) and with more detailed calculations based on a vortex blob method indicate that the flow model is fairly accurate. The discrepancy between the calculated and measured values of the absorption is suspected to be due to the translation of the two-dimensional results into a three-dimensional situation. The procedure proposed by Disselhorst & van Wijngaarden (1980) is based on a matching of the acoustic potential flow. This procedure neglects the contribution of the vortex filament curvature to the self-induced velocity in the three-dimensional case. In the case of a free vortex ring with a core radius corresponding to δ_{ac}, this would result into an underestimation of the vortex velocity by a factor 3. As the vortex ring velocity depends only weakly on the core radius, this effect is only weakly dependent on the frequency.

For low Strouhal numbers, a quasi-steady theory like the one described by Disselhorst & van Wijngaarden (1980) can be used, in which jet flow is assumed during the part of the period of the acoustic field with a positive velocity, and during the remainder of the period the flow is characterized by the formation of a venacontracta with a turbulent recovery region. For the acoustic power absorbed by the vortex shedding non-dimensionalized with $\frac{1}{2}\rho\hat{u}_{ac}^3\pi a^2$ and averaged over a period of the acoustic oscillation, it is found that

$$\bar{P}_{ac}^* = \frac{P_{rad}}{\frac{1}{2}\rho_0 \hat{u}_{ac}^3 \pi a^2} = \beta Sr_{ac}^{\frac{1}{3}} \tag{26}$$

for $Sr_{ac} \gg 1$, where a star denotes the non-dimensionalized quantity, and

$$\bar{P}_{ac}^* = 2c_d/3\pi \tag{27}$$

for $Sr_{ac} \ll 1$. The parameter c_d is determined by the geometry of the pipe end and is equal to 2 for a thin-walled unflanged pipe end and equal to $\frac{13}{9}$ for a flanged pipe. Disselhorst & van Wijngaarden (1980) determined the parameter β by means of numerical simulation and found values between 0.6 and 1.0, depending on the number of point vortices used to describe the vortex shedding process. Using a simpler flow model, but the same procedure to translate the two-dimensional results into the three-dimensional case, Peters & Hirschberg (1993) found a value of $\beta = 0.2$. The power loss due to vortex shedding and radiation of acoustic energy at the pipe end, averaged over

a period, can be determined experimentally from the reflection coefficient using the relation (see Cargill 1982*a*)

$$\bar{P} = \frac{\pi a^2}{2\rho_0 c_0}(|p_+|^2 - |p_-|^2) \tag{28}$$

for an open end in a quiescent fluid. The amplitude of the acoustic velocity $\hat{u}_{ac}$ at the open pipe end can be obtained from $|p_+ - p_-| = \rho_0 c_0 \hat{u}_{ac}$. For low Helmholtz numbers ka the theoretical reflection coefficient for a sharp-edged pipe end without vortex shedding is given by (22). The acoustic power loss by radiation is then given by

$$\bar{P}^*_{rad} = \tfrac{1}{4} ka Sr_{ac}. \tag{29}$$

For low Helmholtz numbers, the power loss by radiation is negligible compared to the nonlinear losses given by (26), as long as

$$Sr_{ac} \ll (ka)^{-\frac{3}{2}} \tag{30}$$

Employing (28), the total loss of acoustic energy was determined from the pressure reflection coefficient at the pipe exit and the amplitude of the pressure signal at a pressure transducer. For three frequencies (27, 54 and 84 Hz), the acoustic Strouhal number was varied by changing the amplitude of the acoustic velocity $\hat{u}_{ac}$. For these frequencies, the Helmholtz number is very small ($ka = 0.0074$, 0.0145 and 0.0230 respectively), so that the condition for neglecting the radiation losses, given by (30), is certainly justified. Figure 12(*a*) compares the experimental data for the non-dimensionalized acoustic power loss by vortex shedding with the predictions of Disselhorst & van Wijngaarden (1980), given by (26) and (27). Also included in figure 12(*a*) are data obtained by Disselhorst & van Wijngaarden (1980) from measurements of the quality factor of a resonating open pipe. Our measured data present an independent check for the theory. It is interesting to note that the high-amplitude data ($Sr_{ac} \ll 1$) agree better with the theory than the original data of Disselhorst & van Wijngaarden (1980). From figure 12(*a*) it is concluded that a quasi-stationary limit for the nonlinear power absorption is found which, for $Sr_{ac} \ll 1$, is very close to the value from the theory proposed by Disselhorst & van Wijngaarden (1980). For lower acoustic amplitudes ($Sr_{ac} \gg 1$) the locally two-dimensional approximation of the vortex shedding proposed by Disselhorst & van Wijngaarden (1980) predicts the functional dependence on Sr_{ac} of the acoustic power. A fair agreement is found for a value $\beta = 0.5$. Hence with $\beta = 0.5$, (26) can be used as a fit of the data for $Sr_{ac} \gg 1$.

A change in the dependence on Sr_{ac} of $\bar{P}^*_{ac}$ is observed around $Sr_{ac} = 10$. This is apparently related to the increasing asymmetry in the flow pattern during inflow and outflow of the acoustic field, observed by Disselhorst & van Wijngaarden (1980) in their flow visualization at $Sr_{ac} \approx 10$.

An advantage of the measurement of the reflection coefficient over the measurement of the quality factor of the resonating pipe used by Disselhorst & van Wijngaarden (1980) to determine the energy absorption by vortex shedding, is that with the present method the influence of the nonlinear behaviour on the end correction can also be determined. From the end correction data shown in figure 12(*b*), it is observed that δ/a varies only slightly with the acoustic Strouhal number. In the high-amplitude limit ($Sr_{ac} \ll 1$), a slight increase (5%) is found relative to the linear behaviour, and a local increase of about 5% is observed around $Sr_{ac} \approx 3$. This rather small influence of flow separation on the end correction is quite surprising when compared to the spectacular effect of a mean flow on the end correction which will be discussed in the following section.

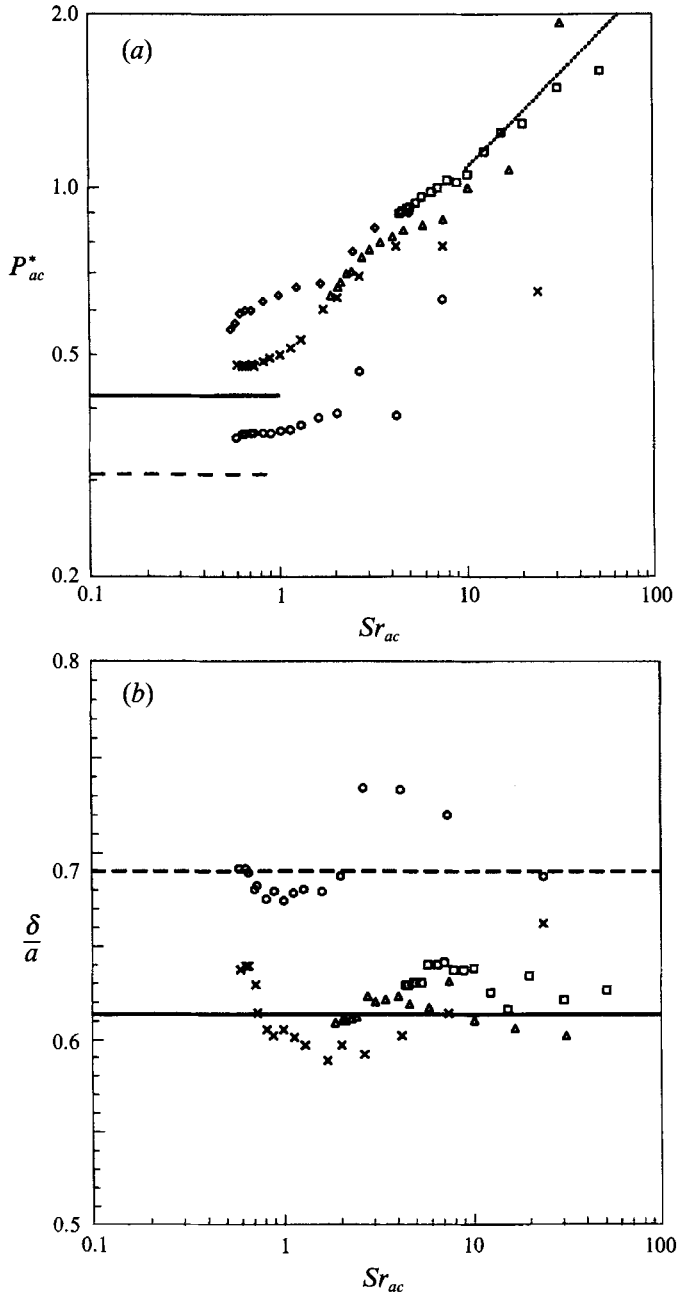

FIGURE 12. Acoustic amplitude dependence of (*a*) the non-dimensionalized acoustic power loss $\bar{P}^*$ and (*b*) the end correction δ in the absence of mean flow for an open pipe end with sharp edges or thick walls. The two-microphone method was used with microphones at positions $x_1 = -86.8$ mm, $x_2 = -224.7$ mm using an experimentally determined value of α_0. Sharp edges $a/(a+d) = 1.00$: ×, $ka = 0.00742$; Δ, $ka = 0.0145$; □, $ka = 0.0230$; ◇, data of Disselhorst & van Wijngaarden (1980). Thick walls $a/(a+d) = 0.70$: ○, $ka = 0.00742$. Theory: (*a*) ——, quasi-stationary theory for $a/(a+d) = 1.00$ (equation (27)); ....., high-frequency limit for $\beta = 0.5$ (equation (26)); – – – –, quasi-stationary theory for $a/(a+d)) = 0.70$ (equation (27)). (*b*) ——, end correction for $a/(a+d) = 1.00$ (Levine & Schwinger 1948); – – – –, end correction for $a/(a+d) = 0.70$ (Ando 1969).

The same experiments were also performed for a pipe end with thick walls, for which $a/(a+d) = 0.70$. The results are also presented in figure 12(*b*). Similarly to the behaviour of a sharp-edged pipe end, for a pipe end with thick walls a quasi-stationary limit of the acoustic power absorption is found, which agree with the predicted value given in (27) for a flanged pipe. However, a strong dip is observed in the acoustic power absorption at a value of the acoustic Strouhal number close to $Sr_{ac} = 5$. For this Strouhal number, during one period of the acoustic field, the vortices shed at the sharp edge of the pipe end travel over a distance of the order of the wall thickness d. This effect is similar to the gain in acoustical energy for the case of a horn with a mean flow, which will be discussed in the next section. This effect can also be associated with the phenomenon of pipe tone and may play a significant role in the acoustical behaviour of tone holes in woodwinds like a clarinet for which at resonance $Sr_{ac} \approx 1$.

The end correction is found to agree with the theory of Ando (1969) for a thick-walled pipe exit for $a/(a+d) = 0.70$ and it shows only a slight influence of the acoustic amplitude for $Sr_{ac} \ll 1$ and $Sr_{ac} \approx 3$.

5. Open pipe end with mean flow

5.1. *Unflanged pipe termination*

A linear theory for the reflection of plane acoustic waves at a thin-walled, unflanged pipe end has been derived by Munt (1977). The results have been obtained in the form of integral equations which have been solved numerically by Munt (1990). In the presence of a uniform subsonic mean flow (plug flow) and for low acoustic amplitudes ($\hat{u}_{ac}/U_0 \ll 1$) the linear theory predicts the pressure reflection coefficient at the pipe end as a function of the Helmholtz number ka and as a function of the mean flow Mach number M. In the theory of Munt, a Kutta condition is assumed to apply at the edges of the pipe end, which implies a finite velocity and pressure at the edges. In that case, an acoustic disturbance of the jet corresponds to a transfer of acoustic energy into the kinetic energy of the vortical disturbances of the jet shear layers. It is found by Munt (1990) that the magnitude of the pressure reflection coefficient approaches a value of 1.0 for all Mach numbers if the Helmholtz number approaches zero, i.e.

$$\lim_{ka \to 0} |R| = 1 \quad \text{for all } M. \tag{31}$$

The acoustic power loss P is, according to Cargill (1982*a*), given by

$$P = \frac{\pi a^2 |\hat{p}_+|^2}{\rho_0 c_0}((1+M)^2 - |R|^2(1-M)^2), \tag{32}$$

which for the limit $ka \to 0$ can be approximated as

$$\lim_{ka \to 0} P = \frac{\pi a^2 |\hat{p}_+|^2}{\rho_0 c_0} 4M \tag{33}$$

irrespective of the frequency. For $M > 0$, P is always positive.

For intermediate Helmholtz numbers and for $M > 0$ the pressure reflection coefficient reaches a maximum value which lies above 1.0. Cargill (1982*b*) found that this maximum value appears at a Strouhal number of $Sr_0 \approx \pi$. The energy reflection coefficient R_E as given by (8) remains less than 1.0 for all values of the Helmholtz number ka.

For low Helmholtz numbers and low Mach numbers approximate but closed-form solutions of the theory of Munt (1990) have been derived by Cargill (1982*a*, *b*) and by

Rienstra (1983). Cargill (1982) and Rienstra (1983) both distinguish between the case where no Kutta condition is imposed and the case where a full Kutta condition is imposed at the sharp edge of the pipe exit, the latter corresponding to the case considered by Munt (1977, 1990). For the reflection coefficient, Cargill (1982*b*) found the following expressions for $ka \ll 1$:

$$|R|_{NK} \approx \left(\frac{1+M}{1-M}\right)(1-\tfrac{1}{2}(ka)^2), \tag{34}$$

$$|R|_{K} \approx \left|\frac{(1+M)g-1}{(1-M)g+1}\right|(1-\tfrac{1}{2}(ka)^2), \tag{35}$$

where $g = (g_1+ig_2)/M$, and g_1, g_2 are functions of the Strouhal number $Sr_0 = ka/M$ defined in Cargill (1982*b*). The indices $_{NK,K}$ denote the results for the cases without and with a Kutta condition imposed, respectively. The frequency dependence of the reflection coefficient corresponds to the low-frequency behaviour in the absence of mean flow given by (22). For $0 < M \ll 1$ the convective correction factor for $|R|$ can be written as

$$|R| = (1+M\mathscr{A})(1-\tfrac{1}{2}(ka)^2), \tag{36}$$

where the amplification factor $\mathscr{A}_{NK} = 2$ and $\mathscr{A}_K = 2-2g_1/(g_1^2+g_2^2)$ which varies continuously between $\mathscr{A}_K = 0$ for $Sr_0 \to 0$ and $\mathscr{A}_K = 0.90$ for $Sr_0 \to \infty$. It is found from (34) and (35) that

$$\lim_{ka\to 0} |R|_K = 1, \tag{37}$$

$$\lim_{ka\to 0} |R|_{NK} = \frac{1+M}{1-M}. \tag{38}$$

The latter result for $|R|_{NK}$ agrees with the result for the flow through the pipe with zero net acoustic power, given by (32), because in the absence of a Kutta condition at the pipe edges no vortical disturbances are produced at the pipe end.

For the Kutta/no Kutta condition cases Rienstra (1983) confirmed the above limiting behaviour of the reflection coefficient. In addition he obtained an expression for the end correction. Rienstra (1983) found also a non-uniform behaviour of the end correction for $ka \ll 1$, $M \ll 1$. For low frequencies ka, in the limit of vanishing mean flow $M \to 0$, with $Sr_0 = ka/M \to \infty$, for the end correction the same limit value as found by Levine & Schwinger (1948) in the absence of mean flow, i.e.

$$\lim_{M\to 0,\, Sr_0\to\infty} \delta/a = 0.6133 \tag{39}$$

was obtained. For small but finite Mach number, and very low frequencies Rienstra (1983) found

$$\lim_{ka\to 0,\, Sr_0\to 0} \delta/a = 0.2554(1-M^2)^{\frac{1}{2}}. \tag{40}$$

Davies *et al.* (1980) report that the end correction does indeed depend strongly on the frequency. However, since the end correction is presented as a function of the Helmholtz number, rather than as a function of the Strouhal number, the differences in the end correction yield an apparent scatter of the obtained values. In addition, the limit of low Strouhal number is not reached because the data reported by Davies *et al.* (1980) and by Munt (1990) have been obtained for $ka > 0.1$ and $M < 0.3$. In the present experiments, our attention was focused on the range of the Helmholtz number

$0 < ka < 0.06$. By varying the Mach number in the range $0.01 < M < 0.2$, the range of Strouhal numbers covered is $0.05 < Sr_0 < 6$. Here we note that Rienstra (1983) did not expect that the low-Strouhal-number limit of the end correction could be obtained experimentally for any reasonable value of ka and M.

Figure 13 presents the amplification factor $\mathscr{A}$, appearing in the expression for the convective factor of the pressure reflection coefficient (equation (36)) and the end correction as a function of the Strouhal number for three different Mach numbers. The data obtained for these three Mach numbers collapse onto Cargill's (1982*b*) and Rienstra's (1983) predictions if a Kutta condition is assumed at the pipe edge. For the various Mach numbers the maximum value of the reflection coefficient is found to agree with the prediction by Cargill (1982*b*), which is $Sr_0 \approx \pi$. Also the data for the end correction, presented in figure 13(*b*) collapse onto a single curve when presented as a function of the Strouhal number. For high Strouhal number, a limiting value is found which is independent of the Mach number, while for low Strouhal number a limiting value $\delta/a = 0.19$ is found. The latter value is close to the limit $0.2554(1-M^2)^{\frac{1}{2}}$ predicted by Rienstra (1983). The Mach-number dependence predicted by Rienstra (1983), (40), could not be verified experimentally, as this Mach number dependence is, for $M < 0.1$, smaller than the scatter in the data ($\pm 0.02a$ in δ). For low Strouhal number, the difference between the predicted and the experimental value of the end correction might be due to the interaction between the unsteady and the stationary boundary layers as described by Howe (1979*a*). As noticed by Howe (1979*a*), the assumption of a uniform flow, made by Munt (1977, 1990), Cargill (1982*b*) and Rienstra (1983) is only valid if the thickness of the unsteady boundary layer $(2\nu/\omega)^{\frac{1}{2}}$ is large compared to the characteristic length of the gradients in the shear layers of the jet leaving the pipe exit. In a turbulent pipe flow this characteristic lengthscale is the thickness of the laminar sublayer δ_l. In our experiments δ_{ac}/δ_l varied between 0.2 and 3. In this range, for the damping of acoustic waves in a turbulent flow, a transition was observed from a weak coupling between the turbulent flow and the acoustic field towards a strong coupling. A breakdown of the validity of the plug-flow model of Munt (1977) could be expected for $\delta_{ac}/\delta_l \ll 1$. It is therefore surprising that the experimental data do not show any deviation from the theoretical results from Munt (1990) in this region.

It is also surprising that even a low-Mach-number mean flow influences the end correction significantly ($> 60\%$), while nonlinearities, shown in figure 12(*b*), involving the formation of free jets, influence the end correction only slightly ($< 10\%$).

5.2. *Thick-walled pipe end and horn*

For the thick-walled pipe terminations, shown in figure 1(*c*), the end correction is presented in figure 13(*b*). For a wall thickness of $d/a = 4/3$ the end corrections for a high Strouhal number equals the value of the end correction in the absence of flow. For low Strouhal numbers, $\delta/a = 0.19$ is found, which is equal to the value obtained at low Strouhal numbers for the end correction of an unflanged pipe termination. For a very thick-walled pipe end, with $d/a = 20/3$, it is shown in figure 13(*b*) that the end correction as a function of the Strouhal number has a similar appearance as for an unflanged pipe end with thinner walls. For low Strouhal numbers the end correction seems to be independent of the wall thickness of the pipe end. The value for high Strouhal numbers is generally found to agree with the end correction in the absence of flow. For an increasing thickness of the wall at the pipe end the end correction for a flanged pipe termination (equation (25)) given by Nomura *et al.* (1960) is obtained.

The influence of the mean flow on the energy reflection coefficient R_E of a pipe,

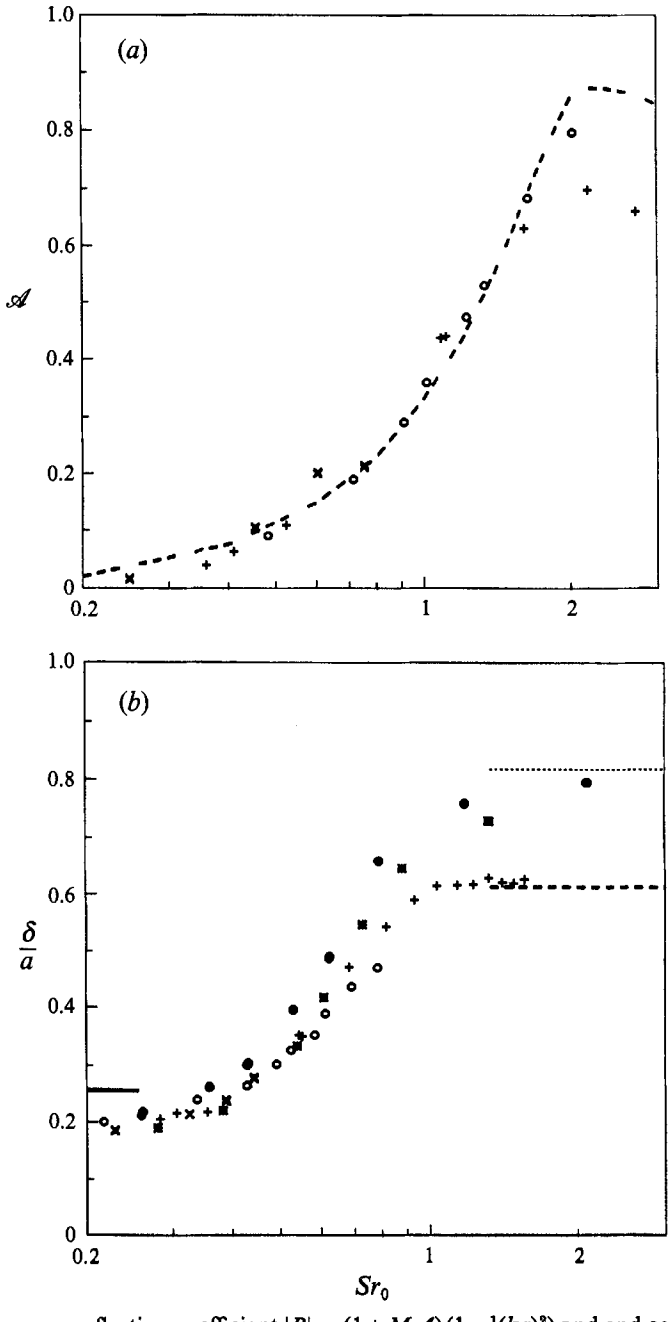

FIGURE 13. Pressure reflection coefficient $|R| = (1+M\mathscr{A})(1-\frac{1}{2}(ka)^2)$ and end correction δ for an open pipe end in the presence of a mean flow at low acoustic amplitudes. Two-microphone method with microphone positions $x_1 = -51.8$ mm, $x_2 = -189.5$ mm, sharp edges: ○, $M = 0.052$, $\hat{u}_{ac}/U_0 \approx 0.1$; +, $M = 0.017$, $\hat{u}_{ac}/U_0 \approx 0.3$. Multi-microphone method with microphone positions $x_1 = -86.9$ mm, $x_2 = -239.3$ mm, $x_3 = -290.1$ mm, $x_4 = -782.4$ mm, $x_5 = -1925.5$ mm. Sharp edges: ×, $M = 0.002$, $\hat{u}_{ac}/U_0 \approx 0.1$. Thick walls: *, $d/a = 4/3$, $M = 0.02$, $\hat{u}_a/U_0 \approx 0.1$; ●, $d/a = 20/3$, $M = 0.01$, $\hat{u}_{ac}/U_0 \approx 0.1$. (*a*) Amplification factor $\mathscr{A}$ as a function of Strouhal number ($Sr_0 = ka/M$): –·–·–·–, $\mathscr{A}_K$, ($\mathscr{A}_{NK} = 2$) (Cargill 1982*b*). (*b*) End correction δ/a as a function of Strouhal number ($Sr_0 = ka/M$). Unflanged pipe end: – – –, Levine & Schwinger (1948) ($M = 0$), and Howe (1979*a*) for $Sr_0 \to \infty$; ——, Rienstra (1983) for $Sr_0 \to 0$. Flanged pipe end: ·····, Nomura *et al.* (1960) ($M = 0$).

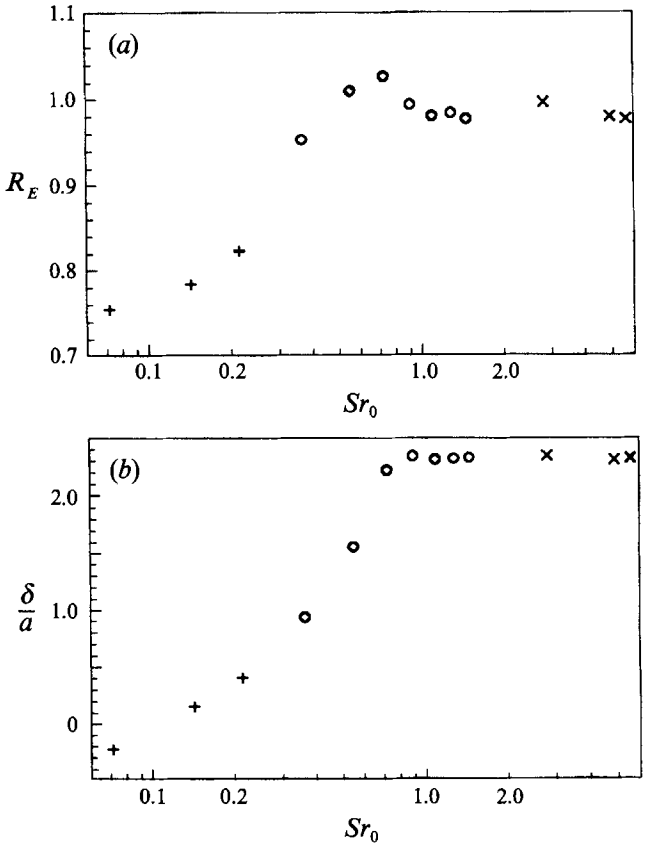

FIGURE 14. (*a*) Energy reflection coefficient R_E and (*b*) end correction δ for a horn as a function of the Strouhal number $Sr_0 = ka/M$. The multi-microphone method was used with microphones at positions $x_1 = -91.8$ mm, $x_2 = -577.8$ mm, $x_3 = -628.8$ mm, $x_4 = -4769.3$ mm, $x_5 = -4964.3$ mm, $x_6 = -6066.8$ mm. +, $M = 0.107$, $\hat{u}_{ac}/U_0 \approx 0.1$; ○, $M = 0.042$, $\hat{u}_{ac}/U_0 \approx 0.1$; ×, $M = 0.011$, $\hat{u}_{ac}/U_0 \approx 0.1$.

terminated by a horn with radius of curvature equal to $r = 4a$ is shown in figure 14(*a*) for the mean flow Mach numbers $M = 0.011$, 0.042 and 0.107. From the comparison with the pressure reflection coefficient obtained in the absence of the mean flow presented in figure 11, it is observed that the reflection coefficient is dramatically influenced by the mean flow. The most striking effect is that, for a limited range of Strouhal numbers around $Sr_0 \approx \pi a/r$, the energy reflection coefficient R_E exceeds a value of 1.0. This indicates that the horn is a source of sound. For a horn such a behaviour has been reported earlier by Powell (1951) from analysing the radiated field and by Hirschberg *et al.* (1988) for different geometries of the horn using a two-microphone method. This feature has been studied by Wilson *et al.* (1971) in connection with human whistling. For the closely related Whistler nozzle configuration a similar behaviour was found by Hirschberg *et al.* (1988), who explained the sound production in terms of vortex sound. Like in the 'Whistler nozzle' studied by Selerowicz, Szumowski & Meier (1991) and Hirschberg *et al.* (1988), the horn presents significant acoustical energy production when the travel time of vortices across the horn matches a number of acoustic oscillation periods. The acoustical energy production at $Sr_0 \approx \pi a/r$ corresponds to the first hydrodynamic mode. A second, less pronounced, maximum at $Sr_0 \approx 2\pi a/r$ corresponds to the second hydrodynamic

mode. This behaviour is a further indication of a strong coupling (Kutta condition) between the acoustic field and the vortical field at the separation point, this in spite of the rather smooth curvature of the wall.

The influence of the mean flow on the end correction is presented in figure 14(*b*). The end correction is measured with the end of the pipe of radius a as reference ($x = 0$). The end correction is dramatically influenced by the mean flow, in a similar manner as found for the unflanged pipe end presented in figure 13(*b*). Similarly to the case of the unflanged pipe the value for high Strouhal numbers corresponds to the data obtained at low amplitudes in the absence of a mean flow (figure 11*b*). For low values of Sr_0 a strong influence of the Mach number on δ is observed. The end correction decreases from the value in the absence of mean flow and for low Helmholtz numbers, $\delta/a = 2.3$, towards a negative value. This strange behaviour of the end correction cannot be explained intuitively and calls for further theoretical analysis. It is also interesting to note that a horn has a more strongly pronounced nonlinear behaviour than an unflanged pipe for $\hat{u}_{ac}/U_0 \approx 0.5$ (Peters *et al.* 1992).

6. Conclusions

A multi-microphone measurement technique is described that is used to obtain accurate values of the reflection coefficient $|R|$ (0.1%), end correction δ ($\pm 0.02a$) and the damping coefficient $\alpha_{\pm}$ (2%) of plane acoustic waves in an open pipe termination for $ka < 0.3$ and $M < 0.2$.

The influence of the room resonances on the measured reflection coefficient $|R|$ is less than 0.2% for $ka < 0.1$ and less than 0.5% for $0.1 < ka < 0.3$. In the absence of a mean flow and for low amplitudes of the acoustic field, the present experimental data for $|R|$, δ and α_0 determined for a closed pipe end and an open sharp-edged pipe end agree with the values provided by the theories proposed by Levine & Schwinger (1948) for $|R|$ and δ, and of the damping α_0 obtained from the solution proposed by Tijdeman (1975). Our data on the influence of the wall thickness on $|R|$ and δ agree with the predictions derived by Ando (1969). For low frequencies $ka \ll 1$ the influence of the wall thickness on the reflection coefficient $|R|$ is found to be negligible. This is in agreement with the conclusion of Bechert (1980), that for low frequencies the exact shape of the pipe exit should not influence $|R|$. However, the end correction δ is strongly influenced by the wall thickness.

For high amplitudes of the acoustic field the influence of vortex shedding predicted earlier by Disselhorst & van Wijngaarden (1980) is confirmed. For low Strouhal numbers Sr_{ac}, based on the amplitude of the acoustic velocity, a quasi-stationary limiting value for the absorbed acoustic power is obtained. For high Strouhal numbers, a locally two-dimensional model of the vortex shedding at the pipe end is used to predict the variation with the Strouhal number of the acoustic power absorption. Application of a two-dimensional model for the vortex shedding process at a circular pipe, as proposed by Disselhorst & van Wijngaarden (1980), yields a prediction of the power absorption which is a factor 2.5 lower than the measurements. This difference might be due to a fundamental problem with the translation from a two-dimensional flow theory to a three-dimensional case. For the high-amplitude behaviour of a pipe end with thick walls an indication was found that for certain values of the Strouhal number Sr_{ac} based on the acoustic velocity and the wall thickness the vortices shed at the pipe end can also transform part of their kinetic energy back into acoustic energy. This behaviour is expected to be signficant in tone holes of reed woodwinds for which at resonance $Sr_{ac} = O(1)$.

For an unflanged pipe end we were able to determine the influence of the mean flow on the behaviour of a sharp-edged pipe termination in a low-amplitude acoustic field. For $M \ll 1$ and $ka \ll 1$ the values predicted by Munt (1990) and Cargill (1982*a*, *b*) for the reflection coefficient and the value predicted by Howe (1979*a*) and Rienstra (1983) for the end correction agree with the values found in the present experiments. For the reflection coefficient, our data confirm the theory of Munt (1990) and Cargill (1982) and therefore indirectly that the Kutta condition has to be imposed at the pipe end. It is surprising that the plug-flow model of Munt (1977) applies so well to a fully developed turbulent mean flow even for values of δ_{ac}/δ_l as low as 0.2. It is shown that the end correction depends mainly on the Strouhal number Sr_0 based on the mean flow velocity, and that for low Strouhal number the end correction tends to the value of $\delta/a = 0.19$, which is close to the value of $\delta/a = 0.2554$ predicted by Rienstra (1983). For high Strouhal numbers Sr_0 the end correction agrees with the theoretical value of $\delta/a = 0.6133$ as predicted by Howe (1979*a*) and Levine & Schwinger (1948). The value of $\delta/a = 0.19$ found for low Strouhal numbers was also obtained for thick-walled pipe ends with $d/a = 4/3$ and $20/3$. A negative value of the end correction was obtained for a pipe terminated by a horn. For all the pipe end geometries studied, the value of the end correction at high Strouhal numbers agreed with the value obtained without a mean flow. On the addition of a mean velocity field, the aero-acoustic behaviour of a horn is considerably influenced in the region where $Sr_0 \approx \pi a/r$. In a critical range of Sr_0 near this value, the energy reflection coefficient R_E is larger than unity.

The influence of the mean flow on the damping coefficient was found to be accurately described by the quasi-laminar theory of Ronneberger (1975) in the region where the ratio $\delta_{ac}/\delta_l < 1$, and by the theory of Howe (1984) in the region where $\delta_{ac}/\delta_l > 1$. The influence of turbulence on the wall shear stress impedance could qualitatively be described by the rigid-plate model, proposed by Ronneberger & Ahrens (1977), modified for inclusion of a memory of the turbulence.

The multi-microphone method is found to be a very useful tool to obtain accurate quantitative data on the effect of vortex shedding on the aeroacoustic behaviour of a pipe termination. Further the influence of imposed unsteadiness on turbulent shear stress can be obtained more accurately using the multi-microphone method than using alternative methods.

This work is part of the Ph.D. thesis by the first author, which is supervised by Professors G. Vossers and H. W. M. Hoeijmakers and has been supported financially by the Netherlands Foundation for Fundamental Research on Matter (FOM project ETN 77.1403) and the N.V. Nederlandse Gasunie. The authors would like also to thank E. Voorthuizen for his permanent support, Dr S. W. Rienstra, Dr J. Kergomard and Dr J. C. Bruggeman for their encouraging comments and Dr D. Ronneberger for some very useful reports. A number of students have contributed to the experimental and theoretical work, and the authors would like to express their thanks to J. A. v.d. Konijnenberg, F. J. J. Huijsmans, G. J. P. ter Horst, P. C. Kriesels, J. Brouwers, R. W. de Leeuw and S. S. op de Beek.

REFERENCES

ABOM, M. & BODEN, H. 1988 Error analysis of two microphone measurements in ducts with flow. *J. Acoust. Soc. Am.* **83**, 2429–2438.

ABRISHAMAN, M. 1977 Effect of flow on the acoustic impedance of a duct exit. *Noise and Fluid Engineering, Proc. Winter Annual Meeting AMSE, Atlanta, Georgia*, pp. 171–177.

ALFREDSON, R. J. & DAVIES, P. O. A. L. 1970 The radiation of sound from an engine exhaust. *J. Sound Vib.* **13**, 389–408.

ANDO, Y. 1969 On the sound radiation from semi-infinite circular pipe of certain wall thickness. *Acustica* **22**, 219–225.

BECHERT, D. W. 1980 Sound absorption caused by vorticity shedding, demonstrated with a jet flow. *J. Sound Vib.* **70**, 389–405.

BODEN, H. & ABOM, M. 1986 Influence of errors on the two-microphone method for measuring acoustic properties in ducts. *J. Acoust. Soc. Am.* **79**, 541–549.

CARGILL, A. M. 1982*a* Low-frequency sound radiation and generation due to the interaction of unsteady flow with a jet pipe. *J. Fluid Mech.* **121**, 59–105.

CARGILL, A. M. 1982*b* Low frequency acoustic radiation from a jet pipe – a second order theory. *J. Sound Vib.* **83**, 339–354.

CUMMINGS, A. 1984 Acoustic nonlinearities and power losses at orifices. *AIAA J.* **22**, 786–792.

CUMMINGS, A. & EVERSMAN, W. 1983 High amplitude acoustic transmission through duct terminations: theory. *J. Sound Vib.* **91**, 503–518.

DAVIES, P. O. A. L. 1987 Plane wave reflection at flow intakes. *J. Sound Vib.* **115**, 560–564.

DAVIES, P. O. A. L. 1988 Practical flow duct acoustics. *J. Sound Vib.* **124**, 91–115.

DAVIES, P. O. A. L., BENTO COELHO, J. L. & BHATTACHARYA, M. 1980 Reflection coefficients for an unflanged pipe with flow. *J. Sound Vib.* **72**, 543–546.

DISSELHORST, J. H. M. & WIJNGAARDEN, L. VAN 1980 Flow in the exit of open pipes during acoustic resonance. *J. Fluid Mech.* **99**, 293–319.

HIRSCHBERG, A., BRUGGEMAN, J. C., WIJNANDS, A. P. J. & MORGENSTERN, M. 1988 The whistler nozzle and horn as aero-acoustic sound sources in pipe systems. *Proc. Inst. Acoust.* **10**, 701–708.

HOWE, M. S. 1979*a* Attenuation of sound in a low Mach number nozzle flow. *J. Fluid Mech.* **91**, 209–229.

HOWE, M. S. 1979*b* The interaction of sound with low Mach number wall turbulence, with application to sound propagation in turbulent pipe flow. *J. Fluid Mech.* **94**, 729–744.

HOWE, M. S. 1984 On the absorption of sound by turbulence and other hydrodynamic flows. *IMA J. Appl. Maths* **32**, 187–209.

INGARD, U. & ISING, H. 1967 Acoustic nonlinearity of an orifice. *J. Acoust. Soc. Am.* **42**, 6–17.

INGARD, U. & SINGHAL, V. K. 1974 Sound attenuation in turbulent pipe flow. *J. Acoust. Soc. Am.* **55**, 535–538.

INGARD, U. & SINGHAL, V. K. 1975 Effect of mean flow on the acoustic resonance of an open-ended duct. *J. Acoust. Soc. Am.* **58**, 788–793.

KIRCHHOFF, G. 1868 Uber den Einfluss der Wärmteleitung in einem Gase auf die Schallbewegung. *Pogg. Ann.* **134** (6), 177–193.

LEVINE, H. & SCHWINGER, J. 1948 On the radiation of sound from an unflanged circular pipe. *Phys. Rev.* **73**, 383–406.

LOUIS, B. & ISABEY, D. 1992 Interaction of oscillatory and constant turbulent flows in airway-like tubes during impedance measurement. *J. Appl. Phys.* (submitted).

MANKBADI, R. R. & LIU, J. T. C. 1992 Near-wall response in turbulent shear flows subjected to imposed unsteadiness. *J. Fluid Mech.* **238**, 55–71.

MECHEL, F., SCHILZ, W. & DIETZ, J. 1965 Akustische Impedanz einder luftdurchstromten offnung. *Acustica* **15**, 199–206.

MORSE, P. M. & INGARD, K. U. 1968 *Theoretical Acoustics*. McGraw-Hill.

MUNT, R. M. 1977 The interaction of sound with a subsonic jet issuing from a semi-infinite cylindrical pipe. *J. Fluid Mech.* **83**, 609–640.

MUNT, R. M. 1990 Acoustic transmission properties of a jet pipe with subsonic jet flow: I, the cold jet reflection coefficient. *J. Sound Vib.* **142**, 413–436.

NOMURA, Y., YAMAMURA, I. & INAWASHIRO, S. 1960 On the acoustic radiation from a flanged circular pipe. *J. Phys. Soc. Japan* **15**, 510–517.

PETERS, M. C. A. M. & HIRSCHBERG, A. 1993 Acoustically induced periodic vortex shedding at sharp edged open channel ends: simple vortex models. *J. Sound Vib.* **161**, 281–299.

PETERS, M. C. A. M., HIRSCHBERG, A., KONIJNENBERG, J. A., HUIJSMANS, F. J. J., LEEUW, R. W. DE,

BEEK, S. S. OP DE & WIJNANDS, A. P. J. 1992 Experimental study of the aeroacoustic behaviour of an open pipe termination at low Mach numbers and low Helmholtz numbers. *AIAA Paper* 90-02-055, Presented at 14th Aeroacoustics Conf. Aachen, Vol. 2, pp. 350–355.

PIERCE, A. D. 1989 *Acoustics, an Introduction to its Physical Principles and Applications*. McGraw-Hill.

POWELL, A. 1951 A Schlieren study of small scale air jets and some noise measurements in two-inch diameter air jets. *ARC* 14726 FM 1694.

RAYLEIGH, LORD 1896 *The Theory of Sound*, vol. II, 2nd edn. Macmillan. 319–326.

RIENSTRA, S. W. 1983 A small Strouhal number analysis for acoustic wave-jet flow-pipe interaction. *J. Sound Vib.* **86**, 539–556.

RONNEBERGER, D. 1975 Genaue Messung der Schalldämpfung und der Phasengeschwindigkeit in durchströmten Rohren im Hinblick auf die Weckselwirkung zwischen Schall und Turbulenz. *Habilitationsschrift Mathematische-Naturwissenschaftliche Fakultät der Universität Göttingen.*

RONNEBERGER, D. 1991 Response of wall turbulence to imposed unsteadiness. *Euromech Colloq.* 272, *Aussois, France.*

RONNEBERGER, D. & AHRENS, C. 1977 Wall shear stress caused by small amplitude perturbations of turbulent boundary-layer flow: an experimental investigation. *J. Fluid Mech.* **83**, 433–464.

SCHLICHTING, H. 1968 *Boundary Layer Theory*. McGraw-Hill.

SELEROWICZ, W. C., SZUMOWSKI, A. P. & MEIER, G. E. A. 1991 Self-excited compressible flow in a pipe-collar nozzle. *J. Fluid Mech.* **228**, 465–485.

TIJDEMAN, H. 1975 On the propagation of sound in cylindrical tubes. *J. Sound Vib.* **39**, 1–33; also *NLR Rep.* MP 74004 U.

TOULOUKIAN, Y. S., SAXENA, S. C. & HESTERMANS, P. 1975 *Thermophysical Properties of Matter.*

WEAST, R. C. 1976 *Handbook of Chemistry and Physics*, 57th edn. CRC Press.

WIJNGAARDEN, L. VAN 1968 On the oscillations near and at resonance in open pipes. *J. Engng Maths* **11**, 225–240.

WILSON, J. A., BEAVERS, G. S., DE COSTER, M. A., HOLGER, D. K. & REGENFUSS, M. D. 1971 Experiments on the fluid mechanics of whistling. *J. Acoust. Soc. Am.* **50**, 366–372.